Bioorganic Chemistry 121 (2022) 105668

Contents lists available at ScienceDirect

Bioorganic Chemistry

journal homepage: www.elsevier.com/locate/bioorg

Revealing 2-dimethylhydrazino-2-alkyl alkynyl sphingosine derivatives as sphingosine kinase 2 inhibitors: Some hints on the structural basis for selective inhibition

Macarena Corro-Morón [a,b], Albert Granell [a], Varbina Ivanova [c], Elena Domingo [d], Raúl Beltrán-Debón [e], Xavier Barril [c,f], Maria-Jesus Sanz [d,g,h], M. Isabel Matheu [a,*], Sergio Castillón [a,*], Yolanda Díaz [a,*]

[a] Departament de Química Analítica i Química Orgànica, Universitat Rovira i Virgili, C/Marcelino Marcel·lí 1, 43007 Tarragona, Spain
[b] R&D Process Development Department, Esteve, C/Caracas 21, 08030 Barcelona, Spain
[c] Facultat de Farmàcia and Institut de Biomedicina, Universitat de Barcelona, Av. Joan XXIII, 27-31, 08028 Barcelona, Spain
[d] Department of Pharmacology, Faculty of Medicine and Odontology, University of Valencia, Av. Blasco Ibáñez 15, 46010 Valencia, Spain
[e] Departament de Bioquímica i Biotecnologia, Universitat Rovira i Virgili, C/Marcelino Marcel·lí 1, 43007 Tarragona, Spain
[f] Catalan Institution for Research and Advanced Studies (ICREA), Passeig Lluís Companys 23, 08010 Barcelona, Spain
[g] Institute of Health Research INCLIVA, University Clinic Hospital of Valencia, Av. Menéndez Pelayo 4, 46010 Valencia, Spain
[h] CIBERDEM-Spanish Biomedical Research Centre in Diabetes and Associated Metabolic Disorders, ISCIII, Av. Monforte de Lemos 3-5, 28029 Madrid, Spain

ARTICLE INFO

Keywords:
Sphingolipids
Sphingosine kinase inhibitors
SphK1
SphK2
Synthesis
Docking
SphK inhibition activity
Cell viability assay

ABSTRACT

Sphingosine kinase (SphK), which catalyzes the transfer of phosphate from ATP to sphingosine (Sph) generating sphingosine-1-phosphate (S1P) has emerged as therapeutic target since the discovery of connections of S1P with cancer progress. So far, most effort has focused on the development of inhibitors of SphK1, and selective inhibitors of SphK2 have been much less explored. Here, we describe the syntheses of new sphingosine derivatives bearing a tetrasubstituted carbon atom at C-2, dimethylhydrazino or azo moieties in the polar head, and alkane, alkene or alkyne moieties as linkers between the polar ahead and the fatty tail. *In vitro* inhibitory assays based on a time resolved fluorescence energy transfer (TR-FRET) have revealed the hydrazino and alkynyl moieties as the best combination for the design of selective SphK2 inhibitors (**19a** and **19b**). Docking studies showed that compounds **19a-b** have the optimal binding to SphK2 through the exploitation of polar but also hydrophobic interactions of their head group with the head of the enzyme binding pocket, while also producing full contact of the fatty tail with the hydrophobic pocket of the enzyme. By contrast, this elongation causes loss of contact surface with the shorter hydrophobic toe of the SphK1 isoform, thus accounting for the SphK2-biased selectivity of these compounds. Cell viability assays of the most promising candidates **19a-b** have shown that **19a** is not cytotoxic to human endothelial cells at 30 μM.

1. Introduction

Over the past three decades, certain sphingolipids, termed bioactive sphingolipids, have been recognized to play important roles in both normal and pathological physiology related to the regulation of cell proliferation, differentiation, survival, trafficking and cell death [1,2]. There are three well-studied bioactive sphingolipids: ceramide (Cer), sphingosine (Sph) and sphingosine-1-phosphate (S1P), which are interconvertible in a complex biosynthetic pathway regulated by specific enzymes (Scheme 1). As a general rule, and opposed to the cellular effects produced by high levels of Cer (apoptosis, senescence, growth arrest, etc.), overproduction of S1P has been associated with proliferation, migration, inflammation, differentiation, survival, effects which, as a whole, can be described as anti-apoptotic [3,4].

Among the family of enzymes involved in the metabolism of sphingolipids, sphingosine kinase (SphK), which catalyzes the transfer of phosphate from ATP to Sph to generate S1P [5], has arisen as a therapeutic target since the discovery of the connections of S1P with cancer progress [3,6,7]. SphK exists in two isoforms, SphK1 and SphK2, which differ in their substrate preferences, subcellular localizations and tissue

* Corresponding authors.
E-mail addresses: maribel.matheu@urv.cat (M.I. Matheu), sergio.castillon@urv.cat (S. Castillón), yolanda.diaz@urv.cat (Y. Díaz).

https://doi.org/10.1016/j.bioorg.2022.105668
Received 3 August 2021; Received in revised form 2 February 2022; Accepted 7 February 2022
Available online 12 February 2022

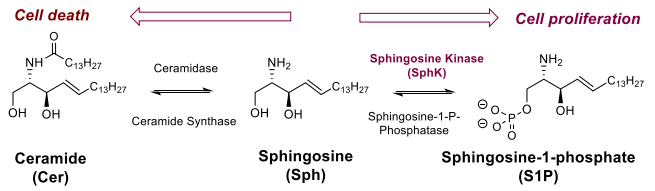

Scheme 1. Sphingolipid rheostat.

distributions, suggesting that they perform different physiological roles [8,9]. SphK1 is located in cytoplasm and after its stimulation by numerous growth factors, cytokines and oncogenes, it is transported to plasma membrane for the phosphorylation of Sph [10]. On the contrary, SphK2 is found in endoplasmic reticulum, mitochondria and nucleus [11]. An overexpression of SphK1 has been associated to cell survival and proliferation [12], and therefore is a key player in cancer [13]. On the contrary, the actions of SphK2 remain poorly understood and much less is known about its biology [14]. Actually, the existing data reveal contradictory actions of SphK2 regarding cancer development [11a,15–18]. Quite recently, the holo structures of SphK1 with Sph and some competitive inhibitors were disclosed, shedding light on the topology and key interactions that govern the ligand-enzyme complex [9,19]. By contrast, no crystal structures are available for SphK2, although structural information on the topology of its binding pocket has been inferred by sequence comparison with SphK1, revealing strong homology to it [8,9,14,20]. These studies suggest that the "*J*-shaped" binding pocket of SphK2 presents a compressed zone at the heel and an expanded surface exhibiting greater plasticity at the toe of the binding pocket, compared to that of SphK1.

SphK inhibitors (SI) have attracted extensive interest for the development of efficient pharmacological therapies against cancer, mainly oriented towards compounds that compete with Sph at the binding pocket of the enzyme [1d,21]. Depending on their specificity against SphK1 or SphK2, SI can be classified as dual or selective inhibitors.

There are many examples of SphK1-selective or SphK1/SphK2-dual inhibitors (Fig. 1). Many of them contain a polar head and a lipophilic tail, mimicking Sph and showing inhibitory potency even in nanomolar range. For example, FTY720 (fingolimod, Gilenya) [22], and (*S*)-FTY720-vinylphosphonate [23], with related structures characterized by the presence of a tetrasubstituted carbon atom at C2 and a benzene ring at the lipophilic tail, are selective SphK1 inhibitors. Other compounds such as Genzyme 51 [24], Amgen 82 [19a] or PF453 [25] have displayed potent inhibition against SphK1, acting all of them in the nanomolar range. Nevertheless, some of these compounds are not completely stable *in vivo,* have low anticancer activity *in vitro* or have off-target effects [21a,26].

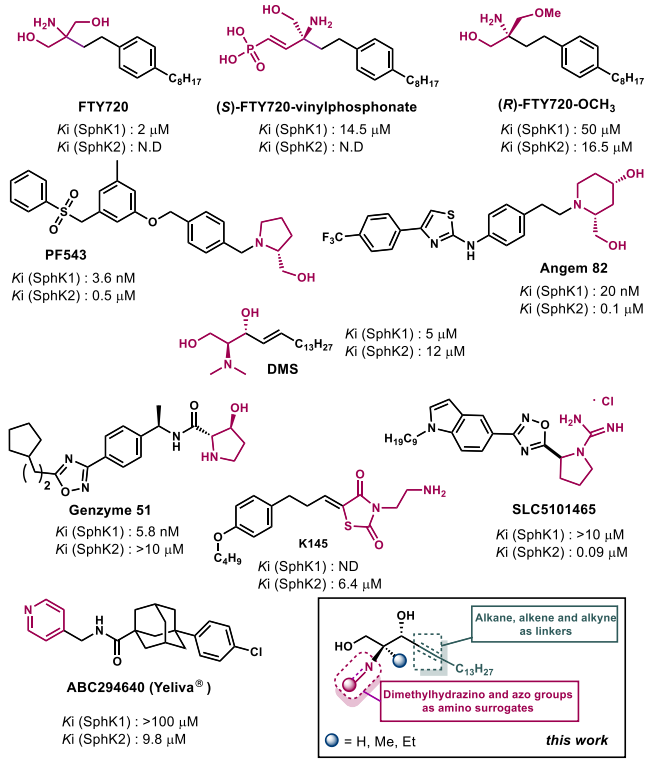

Fig. 1. SphK inhibitors for SphK1 and SphK2 with inhibitory potency.

In comparison with the wide number of SphK1 inhibitors, only a scarce number of SphK2 inhibitors have been described, and most of them display moderate or low selectivity and potency. Among the SphK2 selective inhibitors reported to date, ABC294640 (Yeliva®) is the most advanced and is currently in Phase I/II clinical trials for oncological indications [16]. Other selective SphK2 inhibitors include thiazolidine-2,4-dione K145 [27], and and (*R*)-FTY720-OMe [28].

Compounds containing different nitrogen functional groups [29] including guanidine-[18,20d,30] and amidine-[25,31] moieties have emerged as new potent SphK inhibitors. Modification of the early SphK2 inhibitor SLR080811 [30h] has provided selective SphK2 inhibitors, among which SLC5101465, containing a hydrophobic tail featured with an aliphatic chain attached to a 1,5-disubstituted indole scaffold, a central oxadiazole unit and a guanidine moiety as a polar head (Fig. 1), is the most potent and selective SphK2 inhibitor to date [30a]. The improved biological activity of these derivatives has been ascribed in part to increased interactions of the guanidino moieties with polar amino acids in the active pocket of the SphK.

Based on our previous contributions on the development of synthetic methodologies towards sphingosine and glycolipids [32], we became interested in the design of sphingolipid analogues as potential sphingosine kinase inhibitors. Thus, we recently reported the syntheses of sphingolipid analogues containing a central triazole core, with systematic modifications in the amino functionality and in the fluorination degree of the lipophilic tail [33]. Although these analogues were not superior to *N*,*N*-dimethylsphigosine (DMS) [34a] (Fig. 1), a reference sphingosine-based SphK1/SphK2-dual inhibitor, in terms of inhibitory activity, most of them showed interesting selective SphK2/SphK1 inhibitory profiles. The most SphK2 selective inhibitors resulted from modification of the nitrogen functional group as dimethylamino derivatives, whereas the optimal fluorination degree for SphK2 inhibition was obtained with the heptafluorododecyl tail.

In this study, we sought to investigate the synthesis of sphingosine-based selective SphK2 inhibitors focusing on the following issues:

(1) installation of a non-polar alkyl group at C-2, making it a tetrasubstituted carbon atom, by analogy to (*R*)-FTY720-OCH_3; (2) exploring the role of an alkyne moiety as a rigid linear central linker (and alkene or alkane for comparative purposes) as an alternative to a *p*-phenylene linker, present in many SphK inhibitors; and (3) the presence of unexplored nitrogen functional groups, particularly the dimethylhydrazino group, related to the dimethylamino counterpart in *N*,*N*-dimethylsphigosine (DMS) or in the triazole-based compounds synthesized by us, which might also contribute to increase the highly organised polar interaction network surrounding the polar head (Fig. 1).

2. Results and discussion

2.1. Synthesis of SphK inhibitors

Based on our experience on alkene aziridination [35,36] we envisaged the synthesis of dimethylhydrazino sphingosine analogues by construction of the *anti*-amino alcohol moiety in **A** through the ring-opening reaction of an alkynyl aziridine intermediate **B** (Scheme 2) [37]. The corresponding amino-aziridine intermediate, in turn, could be obtained from the corresponding enynoate **C**, easily available by a

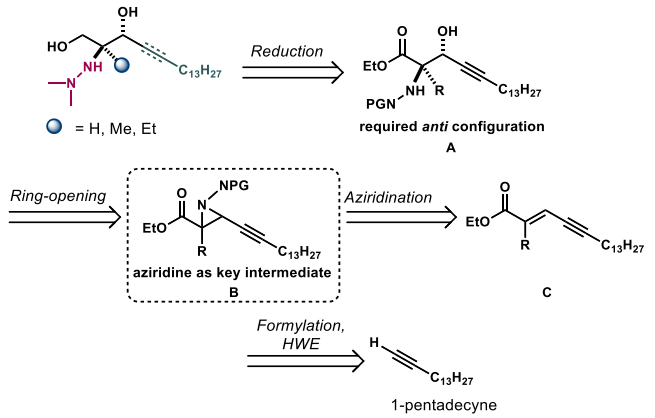

Scheme 2. Retrosynthetic pathway of target sphingosine analogues.

Horner-Wadsworth-Emmons olefination (HWE) [38]. Concomitant reduction of the ester and alkyne groups in **A** would provide the saturated compound. Alternatively, the alkyne moiety can be reduced to an *E* alkene or to a saturated chain (Scheme 2).

Adehyde **2**, afforded from reaction of 1-pentadecyne (**1**) with 1-formylpiperidine, was treated with ethyl 2-(diethoxyphosphoryl)propanoate (**3a**), ethyl 2-(diethoxyphosphoryl)butanoate (**3b**) or ethyl 2-(diethoxyphosphoryl)acetate **3c** in basic medium to provide the corresponding alkenes as *E*/*Z* diastereomeric mixtures in good yields and high *E* stereoselectivities (see experimental section). Column chromatography in silica gel furnished pure *E* alkynes **4a-c** in good isolated yields (Scheme 3) [38].

The configuration in **4a** was determined on the basis of the existence (*Z*) or absence (*E*) of NOE correlations between proton H-3 and the vinylic methyl group (See SI), the configuration of **4b** by analogy with **4a**, and that of **4c** was determined by the coupling constant value of $J = 15.8$ Hz. Aziridines **6a-c** were obtained from **4a-c** in excellent yields and diastereo- and chemoselectivities [39] by reaction with *N*-aminophthalimide as a nitrene precursor and phenyliodide(III) diacetate (PIDA) as oxidant, according to the procedures previously reported by Che [40] and Yudin [41] (Scheme 3). Aziridine **6c** was obtained as a mixture of invertomers (78:22).

Alcohol **5,** available by reduction of **4a** with DIBAL, was also probed as a candidate for amino-aziridination. However, treatment of **5** with *N*-aminophthalimide and $PhI(OAc)_2$ in dichloromethane led to *N*-pththalimidoaziridine **7** in poor yield as a mixture of two invertomers (Scheme 3) [40].

Ring-opening reaction of non-activated aziridines [36a,42] **6a-c** was achieved by treatment with 1.1 equiv of *p*-toluenesulfonic acid (PTSA) in a refluxing 1:1 dioxane-water mixture (Scheme 4). When the reaction was performed in mixtures of water with other solvents (CH_2Cl_2, THF, DMF), or other acids such as $HClO_4$, either the yield decreased or the reaction did not evolve (See Table S1 in SI). Attempts under other reaction conditions, such as 10 mol% of cerium (IV) ammonium nitrate (CAN) in CH_3CN/H_2O [43] or KOH in refluxing DCM led to no conversion or ester hydrolysis, respectively.

In order to assess the effect of the alkyne moiety as a rigid core in the

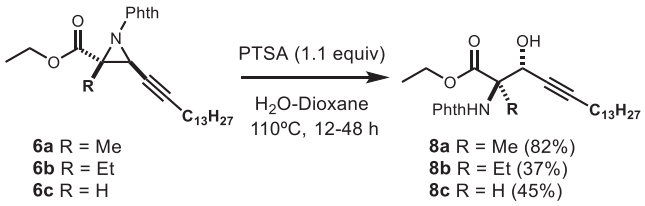

Scheme 4. Ring-opening reaction of aziridines **6a-c**.

inhibitory potency of the sphingosine analogues against SphK, other lipidic tails were also explored, containing either alkene or alkane moieties at the same position. Initial attempts to obtain the corresponding *trans* alkene by partial reduction of **8a** with $LiAlH_4$ at room temperature led to a complex mixture. Fürstner and co-workers had developed a novel *trans* hydroboration [44], hydrogermylation [45], hydrogenation [46], hydrostannation [47] and hydrosilylation [45] of alkynes using ruthenium as catalyst. This methodology was described to be highly *trans* selective and proved to have high functional group tolerance.

To this purpose, compound **8a** was initially submitted to partial hydrogenation with chloro(pentamethylcyclopentadienyl) ruthenium (II) tetramer ($[Cp^*RuCl]_4$), in dichloromethane under 1 bar of hydrogen pressure, but the reaction proceeded in very low conversion.

Hydrosilylation of **8a** with $BnMe_2SiH$ and ($[Cp^*RuCl]_4$) in dichloromethane rendered the alkenylsilane product with only 50% conversion after one hour of reaction. Fortunately, hydrosilylation of **8a** and **8b** with $(EtO)_3SiH$ under similar conditions rendered the corresponding alkenylsilanes **9a-b** in full conversion after 15 min (Scheme 5). The resulting alkenylsilanes **9a-b** were then submitted to protodesilylation with AgF in THF-MeOH, to furnish *trans* **10a** and **10b** in 53% and 63% yield, respectively (Scheme 5, see Table S2 in SI for the whole optimization process) [48].

Furthermore, hydrogenation of **8a** to **11a** was accomplished in very good yield at room temperature under 5 bar of H_2, 30 wt% Pd/C in ethyl acetate as the solvent. Reduction of **8b** required heating at 40 °C to afford **11b** in 78% yield (Scheme 5, see Table S3 in SI for optimization).

Deprotection of phthalamido derivatives **8a-c**, **10a-b** and **11a-b** with methylhydrazine was next explored [49]. Initial reaction of **8a** with

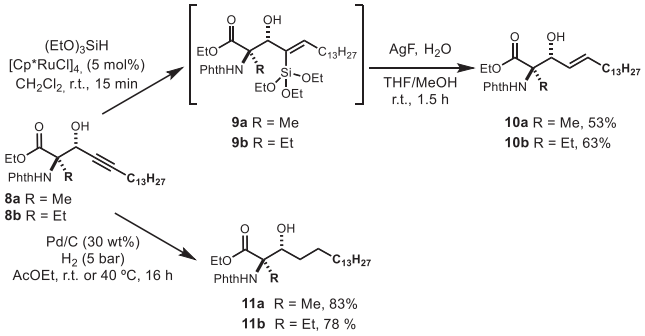

Scheme 5. Reduction of **8a-b** to **10a-b** and **11a-b**.

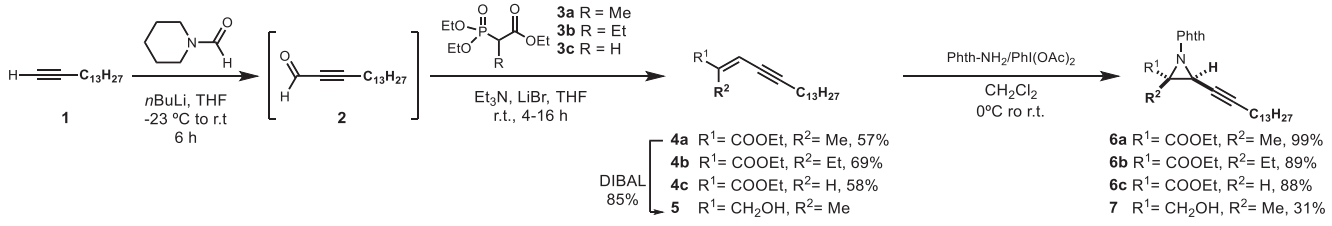

Scheme 3. Synthesis of aziridine derivatives **6a-c** and **7**.

methylhydrazine in THF proceeded with total conversion to render hydrazone **12a**. Structural elucidation of **12a** was based on the following spectroscopic data: (a) the presence of two singlets (3H each) at 1.8 and 1.9 ppm in the ^{1}H NMR spectrum; (b) the presence of a peak at 149.6 ppm in the ^{13}C NMR spectrum, ascribable to an sp^{2} carbon and; (c) the mass spectrum showed a M+ ion 40 units higher than that expected for the free hydrazine derivative. Llebaria and co-workers had already observed a similar behaviour in the synthesis of hydrazines, suggesting that traces of adventitious acetone present in the glassware, laboratory ambient or solvent used favoured the formation of that kind of products [50]. Several attempts with different qualities of solvents and different conditions did not allow us to isolate the free hydrazine. Hence, the hydrazine intermediates obtained by reaction of **8b-c**, **10a-b** and **11a-b** with methylhydrazine were *in situ* treated with acetone at room temperature to render hydrazones **12a-c**, **14a-b** and **16a-b** in good yields (Scheme 6).

Further modification of **12a** via the concomitant reduction of the hydrazone and ester group with $LiBH_4$ to give the hydrazine-based sphingolipid analog resulted unsuccessful. Alternatively, treatment of **12a** with $NaBH_3CN$/AcOH in order to selectively reduce the hydrazone moiety led to a mixture of hydrazino and azo compounds which was used in the next step without further purification (Scheme 6). The formation of the azo moiety was unexpected and very likely resulted from AcOH-mediated isomerization of the hydrazone group, thus making the use of $NaBH_3CN$ unnecessary.

Subsequent treatment of the mixture with DIBAL in dichloromethane at low temperature furnished an *E/Z* mixture of the corresponding azosphingosine analog, which isomerized to the *E* isomer **13a** by stirring overnight in the presence of air and light [51]. In a similar way, compounds **12b-c**, **14a-b** and **16a-b** were transformed into compounds **13b**, **15a** and **17a-b** in moderate to low yield (Scheme 6). Nevertheless, compounds **13c** and **15b** could not be obtained as they presumably decomposed through a *retro*-aldol reaction. *N,N*-Dimethylhydrazino derivatives **18a-c**, **20a-b** and **22a-b** were finally obtained from **8a-c**, **10a-b** and **11a-b** by dephthaloylation to give free hydrazines followed by *in situ* treatment with $NaBH_3CN$ and excess of paraformaldehyde.

Minor amounts of monomethylated and trimethylated products were also detected in all cases. Further reduction of the ester moiety of these compounds with DIBAL provided the *N,N*-dimethylhydrazino sphingosine derivatives **19a-b**, **21b** and **23a-b** in moderate to good yields (Scheme 6). Compounds **19c** and **21a** could not be isolated even though their formation was observed by ^{1}H NMR of their reaction crudes, since they decomposed during the purification.

2.2. In vitro SphK inhibitory activity evaluation

Inhibition potency of the compounds here described were measured by a time resolved fluorescence energy transfer (TR-FRET) procedure that relies on the immunodetection of adenosine diphosphate (ADP) [52,53]. The inhibitory activity was expressed in IC_{50} values. Both SphK1 and SphK2 were examined and DMS was used as a reference inhibitor (Table 1 and Figs. S1 and S2 of SI). Compounds with a saturated fatty tail **17a-b** and **23a-b** did no display inhibitory activity against SphK2 and only **23a** showed a very moderate inhibitory activity against SphK1. However, compounds with insaturations in the skeleton showed IC_{50} close to those determined for us for DMS (SphK1 = 31.5 μM; SphK2 = 9.1 μM), and to those described for ABC294640 (SphK1 < 100 μM; SphK2 ≈ 60 μM)[16] and in general are SphK2-biased inhibitors.

Compounds **13a-b** and **15a** bearing an azo moiety in the polar head proved to be SphK1/SphK2 dual inhibitors. Likewise, compound **21b,** bearing a *N,N*-dimethylhydrazine motif and an alkene as a linker, displayed almost equipotent inhibition of SphK1 and SphK2. However, the combination of an alkyne moiety and a *N,N*-dimethylhydrazino group in **19a** and **19b** led to the most selective SphK2 inhibitors. Unfortunately, we have not been able to assess the effect of a tertiary center in C-2 in the inhibitory potency of these compounds because of the instability exhibited by the synthetic intermediates **13c** and **19c,** preventing access to the corresponding final products. Interestingly, a previous report on sphingosines bearing alkynyl chains with a tertiary center at C-2 showed that the related amino analog displayed little or no inhibition for SphK1 and SphK2, respectively [54].

The selective SphK2 inhibition bias displayed by some of these compounds might be explained by topological changes in the binding pocket of SphK2 related to SphK1. Thus, the replacement of Ile174 and Met272, flanking the surface of the throat of the binding pocket of SphK1, with Val and Leu5 in SphK2, has been suggested to produce a re-contouring of this area of the J-channel, probably making it slightly

Table 1
IC_{50} values are expressed as concentrations (μM). Each value is an average of three experiments. Lower Sphk activity level indicates better inhibition.

Inhibitor	SphK1	SphK2	Inhibitor	SphK1	SphK2
13a	50.4	19.5	**19a**	>200	17.5
13b	43.0	9.8	**19b**	>200	32.5
15a	>70	15.5	**21b**	33.3	29.9
17a	>200	>200	**23a**	72.1	>200
17b	>200	>200	**23b**	>200	>200
DMS	31.5	9.1			

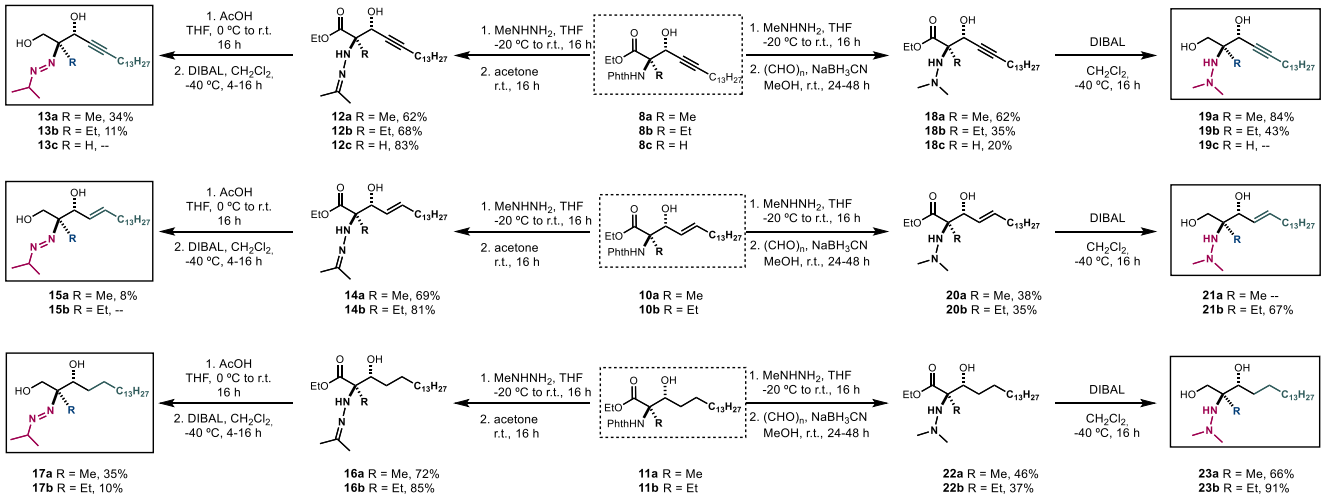

Scheme 6. Synthesis of azo and dimethylhydrazino derivatives **13a-b**, **15a**, **19a-b**, **21b**, **and 23a-b**.

wider in SphK2 than in SphK1. In addition, the replacement of Phe288 in the toe of the hydrophobic pocket of the SphK1 by a Cys in SphK2 results in an extended J-channel [20].

2.3. Docking study

In order to gain insight in the understanding of the SAR information provided by the inhibitory activity assays, we sought to evaluate potential binding modes for a selected group of the compounds synthesized, namely the azo-analogs **13a-b**, the hydrazino SphK2–selective inhibitors **19a-b** and the dual SphK1/SphK2 inhibitor **21b** utilizing a combination of homology modelling and molecular docking. Additionally, compounds featuring a trisubstituted carbon atom at C-2 which either resulted unstable and/or could not be synthesized (**13c** and **19c**, **21c**, R═H), were also prepared for docking in order to elucidate whether their binding modes significantly differ from those of their tetrasubstituted counterparts.

There are 5 X-ray crystal structures of human SphK1 with different inhibitors available in PDB [19] but the SphK2 structure is still unknown. The key residue differences in the binding pocket of the two isoforms are basically Phe288, Ile174, Met272 in SphK1, corresponding to Cys569, Val340 and Leu553 in SphK2 [55]. In addition, Leu553 in SphK2 induces distinct orientational changes in residues Phe358 (Phe192 in SphK1) and Arg357 (Arg191 in SphK1). These structural changes lead to a longer and slightly wider J-shaped pocket in SphK2 [20f]. It has also been reported that enhancing the contacts with the Leu549, the Ser334 and Asp344 of SphK2 around the polar region might lead to a stronger selective inhibition against this isoform [20c].

Calculations were performed using MOE-Dock based on the co-crystal structure of SphK1 with Sph (3VZB, chain A, resolution 2 Å), which was used as a template for the SphK2 homology model after sequence alignment [56] (see details in the experimental section). Independent examination of the docking poses of the two enantiomers of the compounds analysed revealed a better fit of the (2*S*,3*R*) enantiomer in the binding pocket of both the proteins SphK1 and SphK2 (Fig. 2 and details in the Supplementary information).

The best scored binding mode of dual SphK1/SphK2 inhibitor **(2*S*,3*R*)-21b** showed a *J*-shaped conformation of the hydrophobic tail (Fig. 3, ligand in white) and a polar interaction between the dimethylhydrazino group and the Asp178 carboxyl group of SphK1 (Fig. 2. left). This residue also participated in a hydrogen bond with the 3-hydroxyl group, thus making a bidentate interaction with the inhibitor. Additionally, the 3-hydroxyl group was found to form a second H-bond with the structural water molecule next to Ser168 and the 1-hydroxyl group.

Interestingly, the ethyl group at C-2 occupied a hydrophobic region made up by Leu167 and Leu268. This arrangement was found optimal for binding in SphK1 since it led to a maximum number of reasonable interactions between the ligand and SphK1 key residues. Despite the

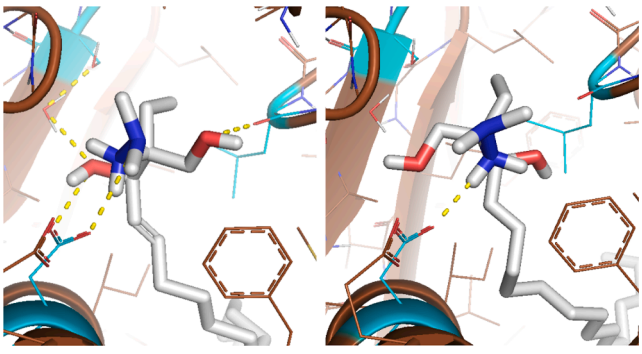

Fig. 2. Binding mode of **(2*S*,3*R*) 21b** enantiomer (left) and **(2*R*,3*S*) 21b** enantiomer (right) in SphK1.

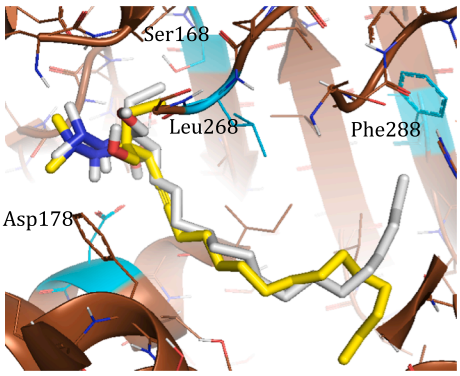

Fig. 3. Docking poses of (2*S*,3*R*) enantiomers of ligands **21b** (white) and **19b** (yellow) in SphK1.

differences in the J-channel shape of SphK2 with respect SphK1, the most probable binding mode of **21b** in SphK2 remained similar to that found by docking in SphK1, thus accounting for the dual inhibitory activity of this compound (Fig. 4, ligand in blue).

Unlike **21b**, the docking poses of compounds **19a** and **19b** in SphK1 showed that their lipophilic tail becomes stiffer and longer due to the presence of a linear triple bond as linker. The tail's elongation apparently leads to a conflict between the ligands and Phe288 at the toe of the binding pocket of SphK1, causing them to enter deeper into the polar region and, thus, losing key interactions with the protein (Fig. S5. left in the Supplementary information (ligand in yellow). In the case of poses with probable binding sites at the head of SphK1, the tail was unable to fit into the cavity and folded, causing a loss of contact surface area with the protein (i.e. loss of hydrophobic interactions) (Fig. 3, ligand in yellow). These observations might explain the lack of SphK1 inhibition by **19a** and **19b**. By contrast, docking analysis of compounds **19a** and **19b** in SphK2 revealed that the elongated ligands preserved the binding mode of compounds **21a-b** by the better fitting of the lipophilic tail in the longer SphK2 toe (Fig. 4, ligand in pink).

The effect of the substitution of carbon at C-2 was studied by docking compounds **19c** and **21c**, having a trisubstituted C-2. The docking poses of these compounds showed a wide variety of possible binding modes, which may be indicative of a heterogeneous binding mode, while the tetrasubstituted C-2 based analogs **19a-b** and **21a-b** showed preference for a particular binding mode with a more extensive network of interactions. The alkyl group, with its tendency to occupy the only hydrophobic region around the head and its bulk, appears to help orient the polar groups into suitable positions for interactions with the enzyme.

The dual inhibitory effect of azo-compounds **13a** and **13b** presented an inconsistency in the presented theory; therefore, they were also

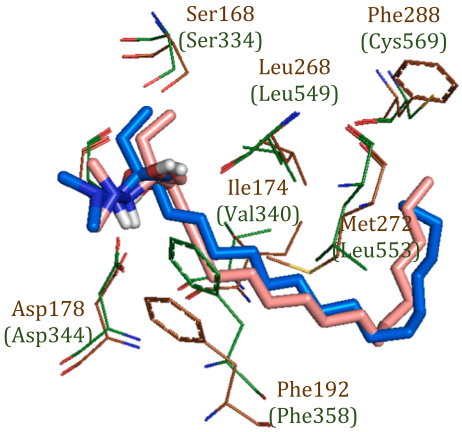

Fig. 4. Docking poses of **(2*S*,2*R*)-21b** (blue) and **(2*S*,3*R*)-19b** (pink) in SphK2.

docked in SphK1. The docking showed that the polar azo head was able to go deeper into the J-channel's head, leaving more space for the elongated lipophilic tail in the cavity and fitting into the smaller SphK1 pocket (See Supplementary information for more detail on this respect).

Collectively, these results suggest that **19a-b** have the optimal binding to SphK2 through the exploitation of polar but also hydrophobic interactions of their head group with the head of the enzyme binding pocket, while also producing full contact of the fatty tail with the hydrophobic pocket of the enzyme. This better fit appears to be due to the presence of a linear alkyne moiety, which further extends the fatty tail deep in the extended hydrophobic pocket of SphK2. By contrast, this elongation causes loss of contact surface with the shorter hydrophobic toe of the SphK1 isoform, thus accounting for the SphK2-biased selectivity of these compounds.

2.4. Cell viability assay

Given that compounds **19a** and **19b** exerted the most relevant effects, they both were primarily tested at 10, 30 and 100 μM for potential cytotoxic effects on primary cell cultures of human umbilical vein endothelial cells (HUVECs).

The studies showed that compound **19a** was not cytotoxic to human endothelial cells at 30 μM either by a cytofluorimetric assay to determine apoptosis and survival (Fig. 5A and 5B) or by the MTT (3[4,5-*dimethylthiazol-2-yl*]-2,5-diphenyltetrazolium bromide) colorimetric assay (Fig. 6A). However, at 100 μM, compound **19a** resulted completely cytotoxic, with a calculated EC_{50} toxicity value (63.12 μM) that is 3.6 fold higher than its inhibitory IC_{50} value (17 μM). Moreover, compound **19b** caused cell damage at at 30 μM in both assays (Fig. 5C and D and Fig. 6B).

3. Conclusions

We have prepared a novel library of sphingosine derivatives with the following structural features: (a) a polar head bearing a tetrasubstituted carbon atom at C-2 and azo or dimethtylhydrazine moieties, and (b) an alkyne, alkene or alkane moieties as a linker with the lipidic tail. We have evaluated these compounds as sphigosine kinase inhibitors, with special focus on the SphK2 *versus* SphK1 inhibition selectivity.

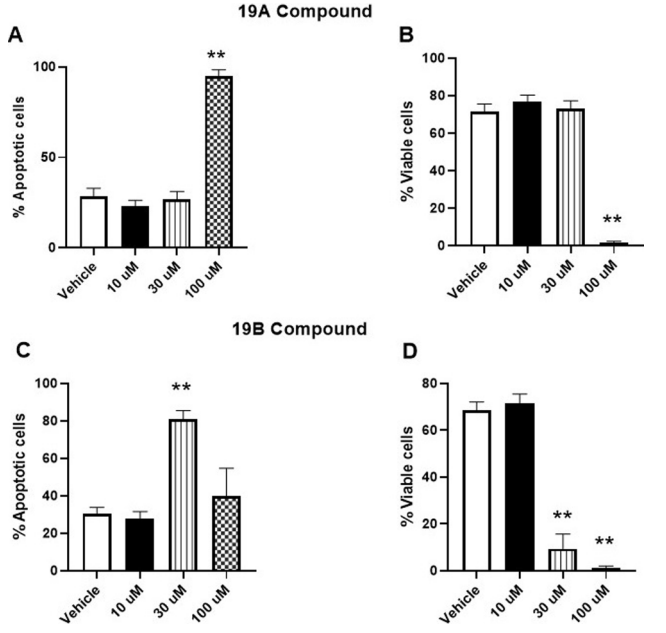

Fig. 5. Effect in percentage of Compound **19a** and **19b** on HUVEC viability and apoptosis. (A) Percentage of apoptotic HUVECs (B) survival HUVEC after 24 h incubation with compound **19a**. (C) Percentage of apoptotic HUVECs (D) survival HUVEC after 24 h incubation with compound **19b**. Apoptotic cells were quantified as the percentage of total population of annexin V+, PI− cells, late apoptotic, and/or necrotic cells as annexin V+, PI+, and viable nonapoptotic cells as annexin V− and PI−. The columns are the mean ± SEM of n = 5 independent experiments. **p < 0.01 relative vehicle group.

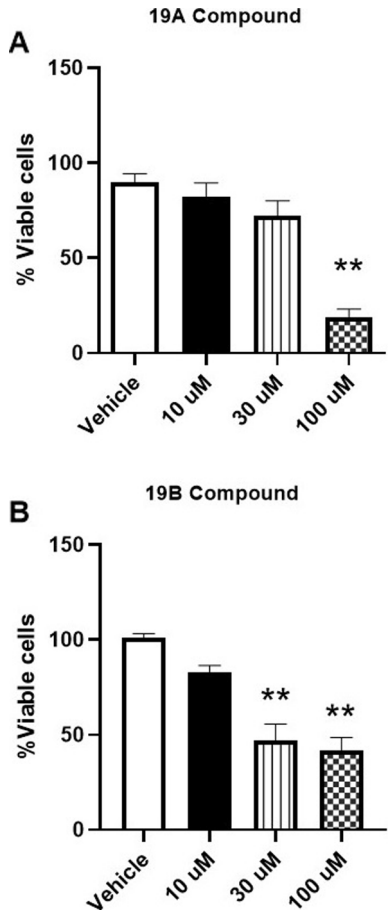

Fig. 6. Effect in percentage of compound **19a** and **19b** on HUVEC viability by MTT assay. Results of the MTT assay for compound **19a** (A) and compound **19b** (B). Columns are the mean ± SEM of n = 5–6 independent experiments. **p < 0.01 relative vehicle group.

In vitro inhibition studies showed that sphingosine derivatives **19a** and **19b** bearing a dimethylhydrazino moiety, a tetrasubstituted carbon atom and an alkynyl linker at C-2 are SphK2-selective inhibitors. In particular, compound **19a** displays inhibition activity against SphK2 in the low micromolar range ($IC_{50} < 20$) with a good selectivity vs SphK1. Docking studies of these compounds into the binding pocket of SphK1 and a homology model of SphK2 have revealed the key interactions that may account for the SphK2-selective inhibition activity. The study revealed a network of polar and unprecedented hydrophobic interactions of the head group of the ligand with the head of the binding pocket and the elongation of the fatty tail deep in the extended hydrophobic pocket of the SphK2 isoform due to the presence of the alkyne linker. In addition, cytofluorimetric assays and MTT colorimetric assays showed that compound **19a** is not cytotoxic to human endothelial cells at 30 μM.

These results still leave room for further optimization but allows considering the use of dimethylhydrazine and the alkyne moieties as structural motifs for the development of selective SphK2 inhibitors. Taking into account that most currently available SphK2 inhibitors developed to date exhibit modest potency and/or low selectivity over SphK1, forthcoming research should redouble efforts on designing compounds that merge high potency with high selectivity in order to

explore the feasibility of SphK2 as a pharmacological target for clinical use.

4. Experimental section

4.1. Chemistry

4.1.1. General methods and synthetic procedures

All reagents were purchased from Sigma Aldrich or Alfa Aesar chemical companies. Dichloromethane (CH_2Cl_2) was distilled from CaH_2, THF was distilled from sodium and Et_3N was stored with activated 4 Å M.S. 4 Å M.S. were activated by heating under high vacuum at 260 °C for 10 h and then were stored at 165 °C. Dioxane, CH_3CN and ethyl acetate were used without any distillation. ^1H and ^{13}C NMR spectra were recorded on a Varian® Mercury VX 400 or on a Bruker® Avance Ultrashield (400 MHz and 100.6 MHz respectively) spectrometer. NMR signals were fully assigned by COSY, HSQC, NOESY and HMBC experiments. All chemical shifts are quoted on the δ scale in ppm using the residual solvent as internal standard (^1H NMR: $CDCl_3$ = 7.26; ^{13}C NMR: $CDCl_3$ = 77.16; ^1H NMR: MeOD = 3.31; ^{13}C NMR: CD_3OD = 49.0). Coupling constants (*J*) are reported in Hz with the following splitting abbreviations: s = singlet, d = doublet, t = triplet, q = quartet, m = multiplet, bs = broad singlet. Infrared (IR) spectra were recorded on a JASCO FTIR-600 plus Fourier Transform Infrared Spectrophotometer, wavenumbers ($\bar{\nu}$) in cm^{-1}. ESI MS were run on an Agilent® 1100 Series LC/MSD instrument. Melting points (m.p.) were recorded with Reichert apparatus. Thin layer chromatography (TLC) was carried out on 0.25 mm E. Merck® aluminium backed sheets coated with 60 F_{254} silica gel. Visualization of the silica plates was achieved using a UV lamp (λmax = 254 nm) and/or by heating plates that were dipped in an anisaldehyde solution. Flash chromatography was carried out using forced flow of the indicated solvent on Fluka® or Merck® silica gel 60 (230–400 mesh). The biological assays were run on a CLARIOstar® BMG LABTECH's instrument using Corning® 384 low volume well plates.

4.1.1.1. General procedure for the preparation of α,β-unsaturated esters ***4a-c*** *[38].* A solution of *n*-BuLi in hexanes (5.28 mmol) was slowly added to a solution of 1-pentadecyne (4.80 mmol) in THF (19.2 mL) at –23 °C. After 2 h, the reaction was allowed to warm at room temperature and it was stirred for other 2 h before cooling at 0 °C. Then, 1-formylpiperidine (5.38 mmol) was added to the pentadecynyllithium suspension at 0 °C and it was stirred at room temperature for 2 h. The reaction was quenched with 20 mL of 10 % aqueous $NaHSO_4$ solution and the product was extracted with Et_2O (4 × 20 mL). The organic layer was washed with 10 % aqueous $NaHSO_4$, dried over anhydrous $MgSO_4$, filtered and concentrated under reduced pressure. The crude alkynal was directly submitted to a Horner-Wadsworth-Emmons olefination without previous purification. To a solution of LiBr (20.90 mmol) in THF (100 mL), the corresponding phosphonate (4.88 mmol) was added at room temperature. After 10 min, Et_3N (6.34 mmol) was introduced into the reaction mixture and it was allowed to stir for 15 min. Then, the freshly synthesized alkynal was dissolved in 20 mL of THF and added to the solution. Once the reaction was completed, the reaction mixture was filtered through silica gel to remove the precipitate formed during the reaction. The pad was washed with 200 mL of hexane/AcOEt 60:40 and the solvent was then removed under reduced pressure. The crude obtained was purified by flash chromatography using hexane/Et_2O (99:1).

4.1.1.2. General procedure to obtain aziridines ***6a-c*** *[57].* A solution of (diacetoxy)iodobenzene (1.50 mmol) in CH_2Cl_2 (2.5 mL) was added to a suspension of *N*-aminophthalimide (2.00 mmol) and the corresponding alkene (1.00 mmol) in CH_2Cl_2 (2.5 mL) at 0 °C. The reaction mixture was stirred at room temperature monitored by TLC until completion. It was then quenched by using a saturated $NaHCO_3$ solution and filtered over celite. The mixture was then extracted with CH_2Cl_2 (3 × 25 mL) and the combined organic layers were dried over anhydrous $MgSO_4$, filtered and concentrated under vacuum. The crude was purified by flash chromatography on silica gel using hexane/AcOEt (95:5).

4.1.1.3. General procedure to afford ring-opened products ***8a-c.*** To a solution of aziridine (0.50 mmol) in dioxane/water 1:1 (6.8 mL), *p*-toluenesulfonic acid (0.55 mmol) was added at room temperature and the reaction mixture was heated under reflux until completion observed by TLC. The mixture was then extracted with Et_2O (3 × 20 mL) and the combined organic layers were dried over anhydrous $MgSO_4$, filtered and concentrated under reduced pressure. The product was purified by flash chromatography using hexane/AcOEt mixtures.

4.1.1.4. General conditions for [ru] catalyzed hydrosilylation of alkynes/protodesilylation to give trans alkenes ***10a*** *and* ***10b*** *[46,58].* In a flame-dried schlenk tube containing a solution of alkyne (0.87 mmol) and $[Cp^*RuCl]_4$ (0.04 mmol) in degassed CH_2Cl_2 (5.0 mL), $(EtO)_3SiH$ (1.57 mmol) was slowly added at room temperature. The resulting mixture was stirred until complete consumption of starting material and the solvent was removed under reduced pressure. Then, a suspension of AgF (0.013 mmol) in a mixture of THF/MeOH/H_2O (5.0:0.3:0.03 mL) was introduced into the schlenck tube and the mixture was stirred for 1.5 h in darkness at room temperature. The solvent was removed under reduced pressure and the crude was purified by flash chromatography using hexane/AcOEt (80:20).

4.1.1.5. General procedure for over-reduction of alkynes to obtain saturated compounds ***11a*** *and* ***11b.*** To a solution of alkyne (0.69 mmol) in AcOEt (22.0 mL) in a Fischer-porter reactor, palladium on carbon (30 mol %) was added. The reactor was then charged with hydrogen (5 bar) and the reaction was stirred at room temperature or 40 °C for 16 h. The reaction mixture was filtered through celite, washed with AcOEt (3x15 mL) and the solvent was removed under reduced pressure. The crude was purified using hexane/AcOEt (80:20).

4.1.1.6. General procedure for hydrazine deprotection and synthesis of hydrazones ***12a-c, 14a-b*** *and* ***16a-b*** *[49].* Methylhydrazine (0.75 mmol) was added to a solution of the *N*-aminophthalimide (0.50 mmol) in THF (3.3 mL) at −20 °C. The solution was stirred at that temperature for 30 min and it was then allowed to warm to room temperature until completion controlled by TLC. The solvent was removed under vacuum and the concentrated crude was redissolved in AcOEt and filtered through cotton to remove the *N*-methyl phthalhydrazide by-product generated during the reaction. Then, the filtrate was evaporated and the residue was redissolved in acetone at room temperature. The solution was stirred until complete formation of the hydrazone and it was then concentrated and purified by flash chromatography.

4.1.1.7. General procedure for formation of azo-sphingosine derivatives ***13a-b, 15a*** *and* ***17a-b.*** To a solution of hydrazone (0.50 mmol) in THF (5.8 mL) at 0 °C, acetic acid (0.95 mmol) was added. Then, the solution was allowed to warm at room temperature and stirred until the starting material was consumed. The reaction was quenched with a saturated solution of $NaHCO_3$ and extracted with AcOEt (3 × 10 mL). The combined organic layers were dried over anhydrous $MgSO_4$, filtered and the solvent was removed under vacuum. The resulting crude containing a mixture of hydrazine and azo- compounds was directly submitted to the next reduction. The crude was redissolved in CH_2Cl_2 (1.2 mL) and the solution was cooled to −40 °C. A solution of DIBAL (1.0 M in dichloromethane, 1.25 mmol) was added dropwise and the mixture was stirred at −40 °C until completion monitored by TLC. Then, the mixture was quenched with a solution of NaOH 1 M, filtered through celite using $CHCl_3$ and extracted with $CHCl_3$ (3 × 5 mL). The combined organic layers were dried over anhydrous $MgSO_4$, filtered and concentrated under reduced pressure. To ensure the formation of *E*-azo-compound,

the crude was allowed to stir in air and in CH_2Cl_2 (2 mL) overnight under light. The crude was purified by silica gel chromatography using hexane/AcOEt mixtures.

*4.1.1.8. General procedure for hydrazine deprotection and further dimethylation to furnish compounds **18a-c, 20a-b** and **22a-b** [59].* Methylhydrazine (0.75 mmol) was added to a solution of the ring-opened products (**8, 10 or 11**) (0.50 mmol) in THF (3.3 mL) at −20 °C. The solution was stirred at the same temperature for 30 min and it was then allowed to warm to room temperature until completion monitored by TLC. The solvent was removed under vacuum and the crude was dissolved in AcOEt and filtered through cotton to remove the *N*-methyl phthalhydrazide by-product generated during the reaction. Then, the filtrate was evaporated and the residue was dissolved in MeOH (13.8 mL). After cooling at 0 °C, $NaBH_3CN$ (1.00 mmol) and paraformaldehyde (2.00 mmol) were added to the reaction mixture and it was then allowed to warm at room temperature and stirred for 24 or 48 h. The solvent was removed under reduced pressure and the crude was dissolved in AcOEt and filtered through a pad of celite. The filtrate was then evaporated and the residue was purified by silica gel chromatography using hexane/AcOEt mixtures.

*4.1.1.9. General procedure to obtain alcohols **5, 19a-b, 21a-b** and **23a-b**.* A solution of DIBAL (1.0 M in dichloromethane, 0.25 mmol) was added dropwise to a solution of alcohol **5** (0.10 mmol) or dimethylhydrazino compounds (**13, 15 or 17**) (0.10 mmol) in CH_2Cl_2 (0.26 mL) at −40 °C. Once the reaction was completed, the mixture was quenched with a solution of NaOH 1 M, filtered through celite using $CHCl_3$ and extracted with $CHCl_3$ (3 × 5 mL). The combined organic layers were dried over anhydrous $MgSO_4$, filtered and concentrated under reduced pressure. The crude was purified by silica gel chromatography using hexane/AcOEt mixtures.

*4.1.2. Ethyl (E)-2-methyloctadec-2-en-4-ynoate (**4a**)*

The reaction was performed as described in general procedure for the synthesis of α,β-unsaturated-esters by using *n*BuLi (2.6 M in hexane, 3.3 mL, 5.28 mmol), 1-pentadecyne (1.26 mL, 4.80 mmol), 1-formylpiperidine (0.6 mL, 5.38 mmol), triethyl 2-phosphonopropionate (1.15 mL, 4.88 mmol), LiBr (1800 mg, 20.90 mmol), Et_3N (0.9 mL) to afford a mixture of esteroisomers *cis/trans* (7:93). After purification using hexane/Et_2O (95:5) the product **4a** (877 mg, 2.74 mmol, 57 % for two steps) was obtained as a yellowish oil. IR (neat): 2924, 2854, 2213, 1713, 1465, 1344, 1258, 1119, 631 cm^{-1}. ^1H NMR (400 MHz, $CDCl_3$) δ 6.61 (m, 1H), 4.19 (q, $J = 7.1$ Hz, 2H), 2.40 (td, $J = 7.0$, 2.2 Hz, 2H), 2.02 (d, $J = 1.3$ Hz, 3H), 1.55 (m, 2H), 1.40 (m, 2H), 1.28–1.20 (m, 21H), 0.87 (t, $J = 6.9$ Hz, 3H). ^{13}C NMR (100 MHz, $CDCl_3$) δ 167.5, 137.9, 120.5, 103.9, 77.7, 60.9, 32.0, 29.9, 29.8, 29.7, 29.6, 29.5, 29.2, 29.0, 28.7, 22.8, 20.0, 15.2, 14.3, 14.2. HR ESI-TOF MS Calculated for [M + Na^+] $C_{21}H_{36}NaO_2^+$ (*m/z*): 343.2608; found: 343.2613.

*4.1.3. (E)-2-methyloctadec-2-en-4-yn-1-ol (**5**)*

Compound **4a** (332 mg, 1.00 mmol) was reacted with DIBAL (2.6 mL, 2.60 mmol, 1.0 M in dichloromethane) in CH_2Cl_2 (2.6 mL) following the procedure described to obtain alcohols. After work-up, the crude was purified using hexane/AcOEt (90:10) to afford **5** (237.8 mg, 0.85 mmol, 85 %) as white solid. m.p. 37–38 °C. IR (neat): 3340, 2922, 2852, 2361, 1464, 1375, 1075, 1014 cm^{-1}. ^1H NMR (400 MHz, $CDCl_3$) δ 5.53 (s, 1.6 Hz, 1H), 4.08 (s, 2H), 2.34 (td, $J = 7.0$, 1.6 Hz, 2H), 1.87 (s, 3H), 1.59–1.49 (m, 2H), 1.46–1.35 (m, 2H), 1.27 (bs, 18H), 0.87 (t, $J = 6.9$ Hz, 3H). ^{13}C NMR (100 MHz, $CDCl_3$) δ 148.3, 105.7, 94.7, 77.61, 67.2, 32.1, 29.8, 29.8, 29.7, 29.5, 29.3, 29.1, 29.1, 22.8, 19.7, 16.4, 14.3. HR ESI-TOF MS for [M + Na^+] $C_{19}H_{34}NaO^+$ (*m/z*): 301.2502; found: 301.2504.

*4.1.4. Ethyl rac-(2R,3S)-[1-(1,3-dioxo-1,3-dihydro-2H-isoindol-2-yl)-2-methyl-3-(pentadec-1-yn-1-yl)aziridine]-2-carboxylate (**6a**)*

Compound **4a** (880.0 mg, 2.74 mmol) was treated with *N*-aminophthalimide (588.6 mg, 5.48 mmol) and (diacetoxy)iodobenzene (1323.8 mg, 4.11 mmol) following the general procedure for aziridination. After the work-up, the crude was purified to obtain aziridine **6a** (1317.0 mg, 100% yield) as a yellow oil. IR (neat): 2927, 2855, 2220, 1715, 1261, 1121, 746, 631 cm^{-1}. ^1H NMR (400 MHz, $CDCl_3$) δ 7.74 (dd, $J = 5.5$, 3.0 Hz, 2H), 7.66 (dd, $J = 5.5$, 3.0 Hz, 2H), 4.14–4.04 (m, 2H), 4.02 (t, $J = 1.8$ Hz, 1H), 2.27 (td, $J = 7.1$, 1.8 Hz, 2H), 1.74 (s, 3H), 1.59–1.48 (m, 2H), 1.44–1.33 (m, 2H), 1.33–1.22 (bs, 18H), 1.19 (t, $J = 7.1$ Hz, 3H), 0.87 (t, $J = 6.9$ Hz, 3H). ^{13}C NMR (100 MHz, $CDCl_3$) δ 167.2, 164.5, 134.1, 130.4, 123.2, 87.0, 72.8, 62.4, 49.9, 43.9, 32.0, 29.8, 29.6, 29.5, 29.2, 29.0, 28.5, 22.8, 19.0, 15.5, 14.3, 14.0. HR ESI-TOF MS Calculated for [2 M + Na^+] $C_{58}H_{80}N_4NaO_8^+$ (*m/z*): 983.5868; found: 983.5875.

*4.1.5. Ethyl rac-(2R,3R)-2-((1,3-dioxo-1,3-dihydro-2H-isoindol-2-yl) amino)-3-hydroxy-2-methyloctadec-4-ynoate (**8a**)*

Compound **8a** was prepared following the general procedure for the ring-opening aziridines, starting from alkynylaziridine **6a** (1300.0 mg, 2.70 mmol) and *p*-toluensulfonic acid (511.4 mg, 2.97 mmol). After the work-up, the crude was purified by flash chromatography by using hexane/AcOEt (from 9:1 to 4:1) to give **8a** as a yellow oil (1102.0 mg, 2.21 mmol, 82 %). IR (neat): 3448, 3230, 2924, 2853, 2223, 1788, 1725, 1466, 1378, 1259, 713, 631 cm^{-1}. ^1H NMR (400 MHz, $CDCl_3$) δ 7.86 (dd, $J = 5.4$, 3.1 Hz, 2H), 7.76 (dd, $J = 5.4$, 3.1 Hz, 2H), 5.77 (s, 1H), 4.42 (dt, $J = 10.9$, 2.0 Hz, 1H), 4.38–4.18 (m, 2H), 4.19 (d, $J = 10.9$ Hz, 1H), 2.17 (td, $J = 7.1$, 2.0 Hz, 2H), 1.52–1.40 (m, 2H), 1.39 – 1.17 (m, 26H), 0.87 (t, $J = 6.8$ Hz, 3H). ^{13}C NMR (100 MHz, $CDCl_3$) δ 172.2, 167.8, 134.7, 129.9, 123.9, 87.4, 77.5, 68.2, 67.8, 62.2, 32.0, 29.8, 29.7, 29.6, 29.5, 29.2, 28.9, 28.6, 22.8, 18.8, 17.4, 14.3, 14.2. HR ESI-TOF MS Calculated for [M + Na^+] $C_{29}H_{42}N_2NaO_5^+$ (*m/z*): 521.2986; found: 521.2982.

*4.1.6. Ethyl rac-(2R,3R,4E)-(2-((1,3-dioxo-1,3-dihydro-2H-isoindol-2-yl) amino)-3-hydroxy-2-methyloctadec-4-enoate (**10a**)*

Compound **10a** was synthesized following the general procedure for hydrosilylation/desilylation from alkyne **8a** (435 mg, 0.87 mmol), $[Cp^*RuCl]_4$ (11.8 mg, 0.04 mmol), CH_2Cl_2 (5 mL), $(EtO)_3SiH$ (0.29 mL, 1.57 mmol). Then, a suspension of AgF (166 mg, 0.013 mmol) in a mixture of THF/MeOH/H_2O (5.0:0.3:0.03 mL) were added. Purification by flash chromatography afforded compound **10a** (230.9 mg, 0.46 mmol, 53%) as a yellow oil. IR (neat): 3461, 3296, 2922, 2852, 2368, 2324, 1788, 1722, 1467, 1378, 1260, 1200, 1104 cm^{-1}. ^1H NMR (400 MHz, $CDCl_3$) δ 7.91–7.82 (m, 2H), 7.82–7.74 (m, 2H), 5.81–5.67 (m, 2H), 5.62 (dd, $J = 15.5$, 5.9 Hz, 1H), 4.35–4.16 (m, 2H), 4.06–3.99 (m, 2H), 2.03 (m, 2H), 1.42–1.16 (m, 28H), 0.87 (t, $J = 6.8$ Hz, 3H). ^{13}C NMR (100 MHz, $CDCl_3$) δ 172.8, 168.0, 135.3, 134.7, 129.9, 127.5, 123.8, 77.2, 68.1, 62.0, 32.4, 32.0, 29.8, 29.7, 29.6, 29.4, 29.3, 29.1, 22.8, 17.7, 14.2. HR ESI-TOF MS Calculated for [M + Na^+] $C_{29}H_{44}N_2NaO_5^+$ (*m/z*): 523.3142; found: 523.3142.

*4.1.7. Ethyl rac-(2R,3R)-2-((1,3-dioxo-1,3-dihydro-2H-isoindol-2-yl) amino)-3-hydroxy −2-methyloctadecanoate (**11a**)*

Following the general procedure for the reduction of alkynes, compound **8a** (341.6 mg, 0.69 mmol) in AcOEt (22 mL) was reduced in the presence of palladium on carbon (102.5 mg, 30 wt%) and 5 bar of hydrogen at room temperature. The crude was purified to afford **11a** (286.8 mg, 0.57 mmol, 83 % yield) as a white solid. m.p. 59 °C. IR (neat): 3475, 3325, 2923, 2852, 1800, 1725, 1467, 1378, 1260, 1200 cm^{-1}. ^1H NMR (400 MHz, $CDCl_3$) δ 7.86 (dd, $J = 5.4$, 3.1 Hz, 2H), 7.76 (dd, $J = 5.4$, 3.1 Hz, 2H), 5.67 (s, 1H), 4.34–4.17 (m, 2H), 3.62–3.42 (m, 2H), 1.66–1.52 (m, 2H), 1.34–1.23 (m, 32H), 0.87 (t, $J = 6.8$ Hz, 3H). ^{13}C NMR (100 MHz, $CDCl_3$) δ 173.4, 168.2, 134.7, 130.0, 123.8, 76.0, 68.2, 62.0, 32.2, 32.1, 29.8, 29.7, 29.5, 26.6, 22.8, 17.7, 14.3, 14.2. HR

ESI-TOF MS Calculated for [M + H^+] $C_{29}H_{47}N_2O_5^+$ (*m/z*): 503.3479; found: 503.3479.

4.1.8. Ethyl rac-(2R,3R)-3-hydroxy-2-methyl-2-(2-(propan-2-ylidene) hydrazinyl) octadec-4-ynoate (12a)

The reaction was performed as described in general procedure for synthesis of hydrazones starting from **8a** (250 mg, 0.50 mmol) and methylhydrazine (40 μL, 0.75 mmol) in THF (1.1 mL). After filtration, the resulting crude was redissolved in 3 mL of acetone, stirred for 16 h and purified by flash chromatography using hexane/AcOEt (4:1) to accomplish hydrazone **12a** (63.0 mg, 0.16 mmol, 62 % over two steps) as a colorless oil. IR (neat): 2929, 2850, 2359, 1714, 1262, 1122, 742, 630 cm^{-1}. ^1H NMR (400 MHz, $CDCl_3$) δ 5.57 (bs, 1H), 4.61 (bs, 1H), 4.30–4.09 (m, 3H), 2.17 (td, J = 7.0, 1.8 Hz, 1H), 1.90 (s, 3H), 1.79 (s, 3H), 1.56 (s, 3H), 1.49–1.39 (m, 2H), 1.39–1.15 (m, 23H), 0.87 (t, J = 6.8 Hz, 3H). ^{13}C NMR (100 MHz, $CDCl_3$) δ 173.6, 148.8, 87.3, 77.7, 68.6, 66.2, 61.5, 32.0, 29.8, 29.7, 29.5, 29.3, 29.0, 28.8, 25.5, 22.8, 19.6, 18.8, 15.8, 14.3, 14.2. HR ESI-TOF MS Calculated for [M + H^+] $C_{24}H_{45}N_2O_3^+$ (*m/z*): 409.3425; found: 409.3426.

4.1.9. rac-(2R,3S)-2-((E)-isopropyldiazenyl)-2-methyloctadec-4-yne-1,3-diol (13a)

Following the general procedure formation of azo compounds and ester reduction, compound **12a** (60 mg, 0.15 mmol) was initially treated with AcOH (20 μL, 0.28 mmol) in 4 mL of THF. In a second step, the resulting crude was redissolved in CH_2Cl_2 (0.38 mL) and treated with DIBAL (0.38 mL, 1 M in dichloromethane, 0.38 mmol). The reaction crude was purified by column chromatography using hexane/AcOEt (4:1) to give **13a** (18.7 mg, 0.05 mmol, 34 % over two steps) as a brownish oil. IR (neat): 3380, 2923, 2853, 2362, 1465, 1275, 1041, 749 cm^{-1}. ^1H NMR (400 MHz $CDCl_3$) δ 4.78 (bs, 1H), 4.12 (d, J = 12.0 Hz, 1H), 3.89 (d, J = 12.0 Hz, 1H,), 3.77–3.63 (m, 1H), 3.25 (s, 1H), 2.77 (s, 1H), 2.22 (td, J = 7.1, 2.1 Hz, 2H), 1.50 (m, 2H), 1.43–1.13 (m, 29H), 0.87 (t, J = 6.9 Hz, 3H). ^{13}C NMR (100 MHz, $CDCl_3$) δ 87.9, 77.9, 74.2, 68.8, 68.0, 66.1, 32.0, 29.8, 29.7, 29.5, 29.2, 29.0, 28.7, 22.8, 20.6, 20.5, 18.9, 18.1, 14.3. HR ESI-TOF MS Calculated for [M + H^+] $C_{22}H_{43}N_2O_2^+$ (*m/z*): 367.3319; found: 367.3317.

4.1.10. Ethyl rac-(2R,3R)-(E)-3-hydroxy-2-(2-(propan-2-ylidene) hydrazinyl)-2-methyl-octadec-4-enoate (14a)

The reaction was performed as described in general procedure for synthesis of hydrazones starting from **10a** (225.0 mg, 0.45 mmol) and methylhydrazine (35.3 μL, 0.67 mmol) in THF (3.3 mL). After filtration, the resulting crude was redissolved in 3 mL of acetone, stirred for 16 h and purified by flash chromatography using hexane/AcOEt (9:1) to afford **14a** (122.9 mg, 0.31 mmol, 69 % over two steps) as a colorless oil. IR (neat): 3371, 3312, 2922, 2853, 2367, 2324, 1731, 1463, 1367, 1234, 1142, 1029 cm^{-1}. ^1H NMR (400 MHz, $CDCl_3$) δ 5.69 (dt, J = 15.2, 6.0 Hz, 1H), 5.52 (dd, J = 15.2, 7.5 Hz, 1H), 5.37 (bs, 1H), 4.44–4.27 (m, 2H), 4.25–4.12 (q, J = 7.1 Hz, 2H), 2.04 (m, 2H), 1.90 (s, 3H), 1.77 (s, 3H), 1.42 (s, 3H), 1.41–1.16 (m, 25H), 0.87 (t, J = 6.8 Hz, 3H). ^{13}C NMR (100 MHz, $CDCl_3$) δ 174.5, 147.9, 134.7, 128.1, 78.1, 66.1, 61.2, 32.5, 32.1, 29.8, 29.6, 29.5, 29.3, 25.5, 22.8, 20.7, 15.6, 14.3. HR ESI-TOF MS Calculated for [M + H^+] $C_{24}H_{47}N_2O_3^+$ (*m/z*): 411.3581; found: 411.3585.

4.1.11. rac-(2R,3S)-(E)-2-(2-(propan-2-ylidene)hydrazinyl)-2-methyloctadec-4-ene-1,3-diol (15a)

Following the general procedure formation of azo compounds and ester reduction, compound **14a** (136 mg, 0.33 mmol) was treated with AcOH (37.7 μL, 0.53 mmol) in 3.8 mL of THF. In a second step the resulting crude was redissolved in CH_2Cl_2 (0.83 mL) and treated with DIBAL (0.83 mL, 1 M in dichloromethane, 0.83 mmol). The reaction was quenched and the crude was firstly purified by flash chromatography using $CHCl_3$/MeOH (24:1) and secondly using hexane/AcOEt (4:1) to give **15a** (10.3 mg, 0.03 mmol, 8 % over two steps) as a colorless oil. IR (neat): 3334, 2927, 2852, 2358, 2342, 1716, 1675, 1464, 1261, 1097, 1050 cm^{-1}. ^1H NMR (400 MHz, CD_3OD) δ 5.67 (dt, J = 13.6, 6.5 Hz, 1H), 5.50–5.39 (m, 1H), 4.50 (d, J = 7.1 Hz, 1H), 3.88 (d, J = 11.3 Hz, 1H), 3.74 (d, J = 11.3 Hz, 1H), 3.66 (dt, J = 10.4, 6.5 Hz, 1H), 2.05 (dd, J = 13.5, 6.5 Hz, 2H), 1.48–1.20 (m, 28H), 1.06 (s, 3H), 0.92 (t, J = 6.8 Hz, 3H). ^{13}C NMR (100 MHz, CD_3OD) δ 134.5, 129.8, 76.4, 69.5, 67.0, 33.3, 33.1, 30.8, 30.7, 30.6, 30.5, 30.3, 30.2, 23.7, 20.8, 15.4, 14.4. HR ESI-TOF MS Calculated for [M + Na^+] $C_{22}H_{44}N_2NaO_2^+$ (*m/z*): 391.3295; found: 391.3309.

4.1.12. Ethyl rac-(2R,3R)-3-hydroxy-2-(2-(propan-2-ylidene)hydrazinyl)-2-methylocta-decanoate (16a)

The reaction was performed as described in general procedure for synthesis of hydrazones starting from **11a** (225 mg, 0.45 mmol) and methylhydrazine (35.3 μL, 0.67 mmol) in THF (3.3 mL). After filtration, the resulting crude was redissolved in 2.5 mL of acetone, stirred for 16 h and purified by flash chromatography using hexane/AcOEt (9:1) to give **16a** (133.0 mg, 0.32 mmol, 72 % over two steps) as a colorless oil. IR (neat): 3649, 2961, 2924, 2853, 2362, 1733, 1457, 1260, 1088, 799, 630 cm^{-1}. ^1H NMR (400 MHz, $CDCl_3$) δ 5.32 (s, 1H), 4.18 (q, J = 7.1 Hz, 2H), 3.93 (bd, J = 7.6 Hz, 1H), 3.82 (m, 1H), 1.90 (s, 3H), 1.77 (s, 3H), 1.65–1.52 (m, 1H), 1.51–1.18 (m, 33H), 0.87 (t, J = 6.9 Hz, 3H). ^{13}C NMR (100 MHz, $CDCl_3$) δ 175.0, 147.7, 76.6, 66.2, 61.2, 32.6, 32.0, 29.8, 29.7, 29.5, 26.6, 25.5, 22.8, 20.7, 15.6, 14.3. HR ESI-TOF MS Calculated for $C_{24}H_{49}N_2O_3$ [M + H^+]: 413.3738; found: 413.3729.

4.1.13. rac-(2R,3S)-2-((E)-isopropyldiazenyl)-2-methyloctadecane-1,3-diol (17a)

Following the general procedure formation of azo compounds and ester reduction, compound **16a** (122.9 mg, 0.30 mmol) was treated with AcOH (35.1 μL, 0.49 mmol) in 5.5 mL of THF. In a second step the resulting crude was redissolved in CH_2Cl_2 (0.71 mL) and treated with DIBAL (0.71 mL, 1 M in dichloromethane, 0.71 mmol). The reaction was quenched and the crude was purified by column chromatography using hexane/AcOEt (4:1) to give **17a** (38 mg, 0.10 mmol, 35 % over two steps) as a yellow oil. IR (neat): 3393, 2921, 2852, 2365, 1464, 1378, 1044 cm^{-1}. ^1H NMR (400 MHz, CD_3OD) δ 4.02 – 3.97 (m, 1H), 3.82 (d, J = 11.2 Hz, 1H), 3.69 (d, J = 11.2 Hz, 1H), 3.62 (dt, J = 13.0, 6.5 Hz, 1H), 1.56 (bs, 2H), 1.40 – 1.19 (m, 32H), 1.04 (s, 3H), 0.90 (t, J = 6.9 Hz, 3H). ^{13}C NMR (100 MHz, CD_3OD) δ 76.8, 74.7, 69.6, 67.3, 33.1, 32.0, 30.8, 30.7, 30.6, 30.5, 27.6, 23.8, 20.7, 14.5, 14.2. HR ESI-TOF MS Calculated for $C_{22}H_{47}N_2O_2$ [M + H^+]: 371.3632; found: 371.3643.

4.1.14. Ethyl rac-(2R,3R)-2-(2,2-dimethylhydrazinyl)-3-hydroxy-2-methyloctadec-4-ynoate (18a)

The reaction was carried out as described in general procedure for synthesis of *N,N*-dimethyl hydrazines starting from **8a** (139.4 mg, 0.28 mmol) and methylhydrazine (22.1 μL, 0.42 mmol) in THF (1.8 mL). When the deprotection was finished, the resulting crude was dissolved in MeOH (7.8 mL) and paraformaldehyde (42 mg, 1.4 mmol) was added. Finally, $NaBH_3CN$ (105.6 mg, 1.68 mmol) was added. The crude was purified by flash chromatography using hexane/AcOEt (from 19:1 to 9:1) to give **18a** (69 mg, 0.17 mmol, 62 % over two steps) as a colorless oil. IR (neat): 3615, 3420, 2926, 2855, 2360, 1715, 1456, 1264, 1122, 888, 740, 631 cm^{-1}. ^1H NMR (400 MHz, $CDCl_3$) δ 4.52 (dd, J = 2.5, 1.5 Hz, 1H), 4.29–4.09 (m, 2H), 2.47 (s, 6H), 2.26–2.10 (m, 2H), 1.54–1.39 (m, 5H), 1.39–1.12 (m, 23H), 0.86 (t, J = 6.9 Hz, 3H). ^{13}C NMR (100 MHz, $CDCl_3$) δ 174.3, 87.4, 78.1, 68.0, 66.8, 61.4, 50.1, 32.0, 29.8, 29.7, 29.5, 29.2, 29.0, 28.7, 22.8, 19.4, 18.8, 14.3, 14.2. HR ESI-TOF MS Calculated for [M + H^+] $C_{23}H_{45}N_2O_3^+$ (*m/z*): 397.3425; found: 397.3431.

4.1.15. rac-(2R,3S)-2-(2,2-dimethylhydrazinyl)-2-methyloctadec-4-yne-1,3-diol (19a)

According to the general procedure to obtain alcohols, dimethyl hydrazine **18a** (69 mg, 0.17 mmol) was treated with DIBAL (0.43 mL, 1

M in dichloromethane, 0.43 mmol) in CH_2Cl_2 (0.43 mL). The crude was purified by silicagel chromatography using hexane/AcOEt (from 9:1 to 4:1) to yield **19a** (52.1 mg, 0.15 mmol, 84 %) as a white solid. IR (neat): 3735, 3381, 2953, 2853, 2366, 2354, 2340, 1467, 1042, 749 cm^{-1}. ^1H NMR (400 MHz, $CDCl_3$) δ 4.61 (t, $J = 2.0$ Hz, 1H), 3.82 (d, $J = 11.1$ Hz, 1H), 3.69 (m, 2H), 2.50 (s, 6H), 2.23 (td, $J = 7.1$, 2.0 Hz, 2H), 1.56–1.42 (m, 2H), 1.42–1.17 (m, 20H,), 1.05 (s, 3H), 0.87 (t, $J = 6.8$ Hz, 3H). ^{13}C NMR (100 MHz, $CDCl_3$) δ 87.9, 78.6, 67.0, 66.6, 61.3, 50.7, 32.0, 29.8, 29.7, 29.5, 29.3, 29.1, 28.8, 22.8, 18.9, 18.4, 14.3. HR ESI-TOF MS Calculated for $[M + H^+]$ $C_{21}H_{43}N_2O_2^+$ (*m/z*): 355.3319; found: 355.3321.

4.1.16. Ethyl rac-(2R,3R,4E)-2-(2,2-dimethylhydrazinyl)-3-hydroxy-2-methyloctadec-4-enoate (20a)

The reaction was carried out following the general procedure for the synthesis of dimethyl hydrazines starting from **10a** (131.4 mg, 0.26 mmol) and methylhydrazine (20.7 μL, 0.39 mmol) THF (1.9 mL). When deprotection was completed the reaction crude was dissolved in MeOH (7.2 mL) and paraformaldehyde (31.5 mg, 1.05 mmol) was added. Finally, $NaBH_3CN$ (32.9 mg, 0.52 mmol) was added. The crude was purified by flash chromatography using hexane/AcOEt (from 9:1 to 4:1) to give **20a** (40 mg, 0.10 mmol, 38 % over two steps) as a colorless oil. IR (neat): 3500, 3448, 2922, 2852, 2770, 2367, 1730, 1465, 1370, 1224, 1108 cm^{-1}. ^1H NMR (400 MHz, CD_3OD) δ 5.68 (dt, $J = 14.8$, 6.8 Hz, 1H), 5.48 (dd, $J = 14.8$, 7.2 Hz, 1H), 4.19–4.10 (m, 2H), 4.03 (d, $J = 7.2$ Hz, 1H), 2.41 (s, 6H), 2.04 (m, 2H), 1.42–1.20 (m, 30H), 0.89 (t, $J = 6.9$ Hz, 3H). ^{13}C NMR (100 MHz, CD_3OD) δ 176.0, 135.2, 129.6, 77.4, 68.9, 61.9, 50.1, 33.4, 33.1, 30.8, 30.6, 30.5, 30.3, 30.2, 23.8, 18.5, 14.6, 14.5. HR ESI-TOF MS for $[M + H^+]$ $C_{23}H_{47}N_2O_3^+$ (*m/z*): 399.3581; found: 399.3587.

4.1.17. Ethyl rac-(2R,3R)-2-(2,2-dimethylhydrazinyl)-3-hydroxy-2-methylocta- decanoate (22a)

The reaction was carried out as described in the general procedure for synthesis of dimethyl hydrazines starting from **11a** (150 mg, 0.28 mmol) and methylhydrazine (17.3 μL, 0.33 mmol) THF (2.2 mL). After deprotection completion, the crude was dissolved in MeOH (8.3 mL) and paraformaldehyde (44.7 mg, 1.49 mmol) was added. Finally, $NaBH_3CN$ (112.4 mg, 1.79 mmol) added. The crude was purified by flash chromatography using hexane/AcOEt (from 9:1 to 4:1) to give **22a** (54.4 mg, 0.14 mmol, 46 % over two steps) as a colorless oil. IR (neat): 3735, 3512, 2923, 2853, 2770, 2362, 2342, 1731, 1457, 1107, 735 cm^{-1}. ^1H NMR (400 MHz, $CDCl_3$) δ 4.32–4.22 (m, 2H), 3.64 (dd, $J = 9.9$, 2.0 Hz, $1H_i$), 3.47 (bs, $1H_i$), 2.44 (s, $6H_i$), 1.59 (bs, 2H), 1.52–1.39 (m, 2H), 1.37–1.13 (m, 30H), 0.87 (t, $J = 6.9$ Hz, 3H). ^{13}C NMR (100 MHz, $CDCl_3$) δ 175.8, 75.9, 67.0, 61.1, 50.2, 32.2, 32.1, 29.8, 29.7, 29.5, 26.8, 22.9, 19.6, 14.3. HR ESI-TOF MS for $[M + H^+]$ $C_{23}H_{49}N_2O_3^+$ (*m/z*): 401.3738; found: 401.3735.

4.1.18. rac-(2R,3S)-2-(2,2-dimethylhydrazinyl)-2-methyloctadecane-1,3-diol (23a)

Following the general procedure for reduction of esters dimethyl hydrazine **22a** (50.9 mg, 0.13 mmol) was treated with DIBAL (0.32 mL, 1 M in dichloromethane, 0.32 mmol) in CH_2Cl_2 (0.32 mL)23a. The crude was purified by silica gel chromatography using hexane/AcOEt (4:1) to give **23a** (30.6 mg, 0.09 mmol, 66 %) as a white solid. M.p. 62 °C. IR (neat): 3734, 2921, 2853, 2366, 1457, 1260, 1033, 799, 749 cm^{-1}. ^1H NMR (400 MHz, CD_3OD) δ 3.71 (d, $J = 10.9$ Hz, 1H), 3.55 (m, 2H), 2.48 (s, 6H), 1.59 (bs, 2H), 1.33 (bs, 26H), 0.91 (m, 6H). ^{13}C NMR (100 MHz, CD_3OD) δ 77.2, 65.0, 62.2, 50.5, 33.1, 32.5, 30.8, 30.5, 28.0, 23.8, 18.5, 14.4. HR ESI-TOF MS Calculated for $[M + H^+]$ $C_{21}H_{47}N_2O_2^+$ (*m/z*): 359.3632; found: 359.3631.

4.1.19. Ethyl (E)-2-ethyloctadec-2-ene-5-ynoate (4b)

The reaction was performed as described in general procedure to synthesize α,β-unsaturated esters *n*BuLi (2.6 M in hexane, 3.3 mL, 5.28 mmol), 1-pentadecyne (1.26 mL, 4.80 mmol), 1-formylpiperidine (0.6 mL, 5.38 mmol), triethyl 2-phosphonobutyrate (1.16 mL, 4.88 mmol), LiBr (1800 mg, 20.90 mmol), Et_3N (0.9 mL) to afford a mixture of esteroisomers *cis/trans* (12:88). After purification using hexane/Et_2O (95:5), **4b** (1141 mg, 3.31 mmol, 69 % over two steps) was obtained as a yellow oil. IR (neat): 2923, 2853, 5357, 2212, 1712, 1609, 1463, 1309, 1238, 1129 cm^{-1}. ^1H NMR (400 MHz, $CDCl_3$) δ 6.59 (t, $J = 2.3$ Hz, 1H), 4.20 (q, $J = 7.1$ Hz, 2H), 2.50 (q, $J = 7.5$ Hz, 2H), 2.41 (td, $J = 7.0$, 2.3 Hz, 2H), 1.62–1.49 (m, 2H), 1.49–1.35 (m, 2H), 1.35–1.17 (m, 21H), 1.06 (t, $J = 7.5$ Hz, 3H), 0.88 (t, $J = 6.9$ Hz, 3H). ^{13}C NMR (100 MHz, $CDCl_3$) δ 167.2, 144.0, 120.0, 103.5, 77.4, 60.8, 32.0, 29.8, 29.7, 29.5, 29.3, 29.0, 28.7, 22.9, 22.8, 20.1, 14.4, 14.3, 13.5. HR ESI-TOF MS for $[M + H^+]$ $C_{22}H_{39}O_2^+$ (*m/z*): 335.2945; found: 335.2950.

4.1.20. Ethyl rac-(2R,3S)-[1-(1,3-dioxo-1,3-dihydro-2H-isoindol-2-yl)-2-ethyl-3-(pentadec-1-yn-1-yl)aziridine]-2-carboxylate (6b)

Compound **4b** (1000 mg, 2.90 mmol) was treated with *N*-aminophthalimide (940 mg, 5.80 mmol) and (diacetoxy)iodobenzene (1400 mg, 4.35 mmol) following the general procedure for aziridination. After the work-up, the crude was purified to afford aziridine **6b** (1277 mg, 2.58 mmol, 89 % as a yellow oil. IR (neat): 3337, 2923, 2853, 2360, 1718, 1466, 1377, 1301, 1237, 1153, 705 cm^{-1}. ^1H NMR (400 MHz, $CDCl_3$) δ 7.73 (dd, $J = 5.5$, 3.0 Hz, 2H), 7.65 (dd, $J = 5.5$, 3.0 Hz, 2H), 4.15–4.05 (m, 2H), 4.01 (t, $J = 1.8$ Hz, 1H), 2.32–2.19 (m, 2H), 1.92 (dq, $J = 14.6$, 7.2 Hz, 2H), 1.59–1.47 (m, 2H), 1.44–1.33 (m, 2H), 1.33–1.22 (m, 21H), 1.19 (t, $J = 7.2$ Hz, 3H), 0.87 (t, $J = 6.9$ Hz, 3H). ^{13}C NMR (100 MHz, $CDCl_3$) δ 166.8, 164.5, 134.1, 130.3, 123.1, 86.7, 72.9, 62.3, 54.1, 43.7, 32.1, 29,8, 29.7, 29.5, 29.2, 29.0, 28.5, 23.6, 22.8, 19.0, 14.3, 14.0, 9.8. HR ESI-TOF MS Calculated for $[M + H^+]$ $C_{30}H_{43}N_2O_4^+$ (*m/z*): 495.3217; found: 495.3218.

4.1.21. Ethyl rac-(2R,3R)-2-((1,3-dioxo-1,3-dihydro-2H-isoindol-2-yl) amino)-3-hydroxy-2-ethyloctadec-4-ynoate (8b)

Compound **8b** was prepared following the general procedure for the ring-opening aziridines, starting from **6b** (310.7 mg, 0.628 mmol) and *p*-toluensulfonic acid (131.4 mg, 0.69 mmol). After the work-up, the crude was purified by flash chromatography using hexane/AcOEt (from 9:1 to 4:1) to give product **8b** (122.4 mg, 0.23 mmol, 37 %) as a yellow oil. IR (neat): 3446, 3312, 2924, 2853, 2363, 1725, 1450, 1378, 1237 cm^{-1}. ^1H NMR (400 MHz, $CDCl_3$) δ 7.85 (dd, $J = 5.5$, 3.1 Hz, 2H), 7.76 (dd, $J = 5.5$, 3.1 Hz, 2H), 5.66 (s, 1H), 4.53 (s, 2H), 4.35–4.17 (m, 2H), 2.09 (t, $J = 7.0$ Hz, 2H), 1.96 (dq, $J = 14.8$, 7.4 Hz, 1H), 1.63 (dq, $J = 14.8$, 7.4 Hz, 1H), 1.46–1.34 (m, 2H), 1.34–1.17 (m, 23H), 1.02 (t, $J = 7.4$ Hz, 3H), 0.86 (t, $J = 6.6$ Hz, 3H). ^{13}C NMR (100 MHz, $CDCl_3$) δ 171.5, 168.1, 134.7, 130.0, 123.8, 87.2, 77.6, 71.5, 65.5, 61.9, 32.0, 29.8 , 29.7, 29.5, 29.2, 28.9, 28.6, 24.7, 22.8, 18.8, 14.3, 14.2, 8.3. HR ESI-TOF MS Calculated for $[M + H^+]$ $C_{30}H_{45}N_2O_5^+$ (*m/z*): 513.3323; found: 513.3324.

4.1.22. Ethyl rac-(2R,3R,4E)-2-((1,3-dioxo-1,3-dihydro-2H-isoindol-2-yl) amino)-3-hydroxy-2-ethyloctadec-4-enoate (10b)

Compound **10b** was prepared following the general procedure for hydrosilylation/desilylation from alkyne **8b** (400 mg, 0.88 mmol), $SiH(OEt)_3$ (0.29 mL, 1.57 mmol) and $[Cp^*RuCl]_4$ (12.0 mg, 0.04 mmol) in degassed CH_2Cl_2 (5.4 mL). Then, a suspension of AgF (167 mg, 0.013 mmol) in a mixture of THF/MeOH/H_2O (5.4:0.3:0.03 mL) was added. The crude was purified by flash chromatography to afford **10b** (283.1 mg, 0.55 mmol, 63% for the two steps) as a yellow oil. IR (neat): 3448, 3299, 2922, 2852, 2770, 2367, 2324, 1730, 1465, 1371, 1224, 1108 cm^{-1}. ^1H NMR (400 MHz, $CDCl_3$) δ 7.86 (dd, $J = 5.5$, 3.0 Hz, 2H), 7.77 (dd, $J = 5.5$, 3.0 Hz, 2H), 5.72–5.62 (m, 3H), 4.37 (bs, 1H), 4.27 (q, $J = 7.1$ Hz, 2H), 4.06 (bs, 1H), 2.11–1.95 (m, 2H), 1.85 (dq, $J = 14.6$, 7.3 Hz, 1H), 1.44 (dq, $J = 14.6$, 7.3 Hz, 1H), 1.36–1.19 (m, 25H), 1.04 (t, $J = 7.3$ Hz, 3H), 0.87 (t, $J = 6.9$ Hz, 3H). ^{13}C NMR (100 MHz, $CDCl_3$) δ 171.9, 168.5, 135.4, 134.8, 130.1, 127.7 , 123.9, 75.4, 72.2, 61.8, 32.5, 32.1, 29.8, 29.6, 29.5, 29.3, 29.2, 24.7, 22.8, 14.3, 8.4. HR ESI-TOF MS

Calculated for [M + Na^+] $C_{30}H_{46}N_2NaO_5^+$ (*m/z*): 537.3299; found: 537.3300.

4.1.23. Ethyl rac-(2R,3R)-2-((1,3-dioxo-1,3-dihydro-2H-isoindol-2-yl) amino)-3-hydroxy −2-ethyloctadecanoate (11b)

Following the general procedure for the reduction of alkynes, compound **8b** (241.7 mg, 0.47 mmol) in AcOEt (14.5 mL) was reduced in the presence of palladium on carbon (7.5 mg, 30 wt%) and 5 bar of hydrogen at 40 °C. The crude was purified to afford **11b** (190.0 mg, 0.37 mmol, 78 % yield) as a yellow oil. IR (neat): 3477, 3295, 2922, 2852, 2368, 1788, 1719, 1467, 1377, 1233, 1200 cm^{-1}. ^1H NMR (400 MHz, $CDCl_3$) δ 7.85 (dd, J = 5.5, 3.1 Hz, 2H), 7.75 (dd, J = 5.5, 3.1 Hz, 2H), 5.75 (s, 1H), 4.26 (qd, J = 7.1, 1.2 Hz, 2H), 3.88 (d, J = 9.2 Hz, 1H), 3.68–3.58 (m, 1H), 1.87 (dq, J = 14.6, 7.3 Hz, 1H), 1.77–1.56 (m, 2H), 1.50 (dq, J = 14.6, 7.3 Hz, 1H), 1.44–1.17 (m, 29H), 1.01 (t, J = 7.3 Hz, 3H), 0.86 (t, J = 6.9 Hz, 3H). ^{13}C NMR (100 MHz, $CDCl_3$) δ 172.6, 168.4, 134.7, 130.1, 123.8, 74.0, 71.9, 61.8, 32.2, 32.1, 29.8, 29.50, 26.8, 24.2, 22.8, 14.3, 8.5. HR ESI-TOF MS Calculated for [M + H^+] $C_{30}H_{49}N_2O_5^+$ (*m/z*): 517.3636; found: 517.3641.

4.1.24. Ethyl rac-(2R,3R)-2-ethyl-3-hydroxy-2-(2-propan-2-ylidene) hydrazinyl)octadec-4-ynoate (12b)

The reaction was performed following the general procedure for synthesis of hydrazones starting from **8b** (250 mg, 0.49 mmol) and methylhydrazine (38.5 μL, 0.73 mmol) in THF (3.7 mL). After filtration, the resulting crude was redissolved in 3 mL of acetone, stirred for 16 h and purified by flash chromatography using hexane/AcOEt (9:1) to accomplish **12b** (139.3 mg, 0.32 mmol, 68 % over two steps) as a colorless oil. IR (neat): 3393, 2923, 2853, 2364, 1734, 1463, 1234, 1147, 1028 cm^{-1}. ^1H NMR (400 MHz, $CDCl_3$) δ 5.71 (s, 1H), 5.21 (d, J = 9.1 Hz, 1H), 4.68 (dt, J = 9.1, 7.0 Hz, 1H), 4.28–4.16 (m, 2H), 2.25 (dq, J = 14.9, 7.5 Hz, 1H), 2.16 (td, J = 7.0, 2.0 Hz, 2H), 1.98–1.85 (m, 4H), 1.82 (s, 3H), 1.53–1.38 (m, 2H), 1.37–1.19 (m, 23H), 0.86 (m, 6H). ^{13}C NMR (100 MHz, $CDCl_3$) δ 172.0, 147.9, 87.0, 78.3, 69.7, 69.3, 61.5, 32.0, 29.8, 29.7, 29.5, 29.3, 28.9, 26.3, 25.5, 22.8, 18.9, 15.7, 14.3, 8.41. HR ESI-TOF MS Calculated for [M + H^+] $C_{25}H_{47}N_2O_3^+$ (*m/z*): 423.3581; found: 423.3591.

4.1.25. rac-(2R,3S,4E)-2-ethyl-2-(isopropyldiazenyl)octadec-4-yne-1,3-diol (13b)

Following the general procedure for formation of azo compounds and ester reduction, compound **12b** (139.3 mg, 0.32 mmol) was treated with AcOH (37.6 μL, 0.52 mmol) in THF (3.9 mL). In a second step the resulting crude was redissolved in CH_2Cl_2 (0.83 mL) and treated with DIBAL (0.83 mL, 1 M in dichloromethane, 0.83 mmol) was slowly added. The reaction was quenched and the crude was purified by using CH_2Cl_2/hexane (9:1) to give **13b** (13.9 mg, 0.04 mmol, 11 % over two steps) as a yellowish oil. IR (neat): 3334, 3162, 2923, 2853, 2360, 2327, 1262, 1033, 746 cm^{-1}. ^1H NMR (400 MHz, MeOD) δ 4.80 (s, 1H), 3.96 (d, J = 11.6 Hz, 1H), 3.87 (d, J = 11.6 Hz, 1H), 3.73–3.62 (m, 1H), 2.20 (t, J = 6.7 Hz, 2H), 1.93 (td, J = 15.0, 7.5 Hz, 1H), 1.81 (td, J = 15.0, 7.5 Hz, 1H), 1.57–1.19 (m, 28H), 0.90 (t, J = 6.6 Hz, 3H), 0.81 (t, J = 7.5 Hz, 3H). ^{13}C NMR (100 MHz, MeOD) δ 86.2, 78.4, 75.6, 68.5, 65.0, 62.6, 31.7, 29.4, 29.3, 29.1, 28.8, 28.5, 28.3, 23.4, 22.3, 19.6, 19.5, 18.0, 13.0, 6.2. HR ESI-TOF MS for [M + Na^+] $C_{23}H_{44}N_2NaO_2^+$ (*m/z*): 403.3295; found: 403.3290.

4.1.26. Ethyl rac-(2R,3R,4E)-3-hydroxy-2-(2-(propan-2-ylidene) hydrazinyl)-2-ethyl-octadec-4-enoate (14b)

The reaction was performed as described in general procedure for synthesis of hydrazones starting from **10b** (247 mg, 0.48 mmol) and methylhydrazine (37.9 μL, 0.72 mmol) in 3.5 mL of THF. After filtration, the resulting crude was redissolved in 3 mL of acetone, stirred for 16 h and purified by flash chromatography using hexane/AcOEt (9:1) to accomplish **14b** (165.3 mg, 0.39 mmol, 81 % over two steps) as a colorless oil. IR (neat): 3372, 3325, 2922, 2853, 2354, 2312, 1731, 1463, 1367, 1234, 1142 cm^{-1}. ^1H NMR (400 MHz, $CDCl_3$) δ 5.70–5.59 (m, 1H), 5.54 (dd, J = 15.3, 7.4 Hz, 1H), 5.48 (bs, 1H), 5.09 (bs, 1H), 4.35 (d, J = 7.4 Hz, 1H), 4.19 (q, J = 7.1 Hz, 2H), 2.13 (td, J = 14.8, 7.4 Hz, 1H), 2.06–1.95 (m, 2H), 1.92 (s, 3H), 1.90–1.82 (m, 1H), 1.79 (s, 3H), 1.39–1.17 (m, 25H), 0.87 (t, J = 6.8 Hz, 3H), 0.79 (t, J = 7.4 Hz, 3H). ^{13}C NMR (100 MHz, $CDCl_3$) δ 172.8, 146.4, 134.2, 128.8, 78.6, 69.3, 61.1, 32.4, 32.0, 29.7, 29.6, 29.4, 29.3, 29.2, 26.9, 25.4, 22.7, 15.3, 14.3, 14.2, 8.0. HR ESI-TOF MS Calculated for [M + Na^+] $C_{25}H_{48}N_2NaO_3^+$ (*m/z*): 447.3557; found: 447.3555.

4.1.27. Ethyl rac-(2R,3R)-3-hydroxy-2-(2-(propan-2-ylidene)hydrazinyl)-2-ethylocta-decanoate (16b)

The reaction was performed as described in general procedure for synthesis of hydrazones starting from **11b** (168.7 mg, 0.33 mmol) and methylhydrazine (25.8 μL, 0.49 mmol) THF (2.4 mL). After filtration, the resulting crude was redissolved in 3 mL of acetone, stirred for 16 h and purified by flash chromatography using hexane/AcOEt (9:1) to accomplish **16b** (118 mg, 0.28 mmol, 85 % over two steps) as a yellow oil. IR (neat): 3408, 2921, 2852, 2359, 2842, 1730, 1457, 1367, 1234, 1142 cm^{-1}. ^1H NMR (400 MHz, $CDCl_3$) δ 5.47 (s, 1H), 4.67 (bs, 1H), 4.20 (dq, J = 7.1, 2.8, 2H), 3.87 (d, J = 9.7 Hz, 1H), 2.18 (dq, J = 14.9, 7.5 Hz, 1H), 1.92–1.80 (m, 4H), 1.79 (s, 3H), 1.59–1.43 (m, 2H), 1.37–1.16 (m, 29H), 0.87 (t, J = 6.8 Hz, 3H), 0.76 (t, J = 7.4 Hz, 3H). ^{13}C NMR (100 MHz, $CDCl_3$) δ 173.4, 146.2, 77.0, 69.2, 61.2, 33.6, 32.1, 29.8, 29.5, 27.2, 26.6, 25.6, 22.8, 15.3, 14.3, 8.0. HR ESI-TOF MS Calculated for [M + H^+] $C_{25}H_{51}N_2O_3^+$ (*m/z*): 427.3894; found: 427.3883.

4.1.28. rac-(2R,3S)-2-((E)-isopropyldiazenyl)-2-ethyloctadecane-1,3-diol (17b)

Following the general procedure formation of azo compounds and ester reduction, compound **17b** (126.6 mg, 0.3 mmol) was treated with AcOH (33.8 μL, 0.47 mmol) THF (3.4 mL). In a second step the resulting crude was redissolved in CH_2Cl_2 (0.74 mL) and treated with DIBAL (0.74 mL, 1 M in dichloromethane, 0.74 mmol) was slowly added. The reaction was quenched and the crude was purified by using hexane/AcOEt (95:5) to give **17b** (11.1 mg, 0.03 mmol, 10 % over two steps) as a colorless oil. IR (neat): 3397, 2921, 2852, 2360, 2300, 1727, 1464, 1379, 1049 cm^{-1}. ^1H NMR (400 MHz, CD_3OD) δ 3.92 (dd, J = 10.3, 1.7 Hz, 1H), 3.80 (bs, 2H), 3.65 (dt, J = 13.0, 6.5 Hz, 1H), 1.91–1.74 (m, 2H), 1.51 (m, 2H), 1.44–1.17 (m, 32H, 0.89 (t, J = 6.9 Hz, 3H), 0.78 (t, J = 7.5 Hz 3H). ^{13}C NMR (100 MHz, CD_3OD) δ 77.1, 75.6, 69.9, 64.2, 33.1, 32.3, 30.8, 30.7, 30.5, 27.8, 24.0, 23.8, 20.9, 14.5, 7.8. HR ESI-TOF MS Calculated for [M + H^+] $C_{23}H_{49}N_2O_2^+$ (*m/z*): 385.3789; found: 385.3793.

4.1.29. Ethyl rac-(2R,3R)-2-(2,2-dimethylhydrazinyl)-3-hydroxy-2-ethyloctadec-4-ynoate (18b)

The reaction was carried out as described in general procedure for synthesis of *N,N*-dimethyl hydrazines starting from **8b** (145 mg, 0.28 mmol) and methylhydrazine (22.3 μL, 0.42 mmol) THF (2.1 mL). After deprotection completion the resulting crude was dissolved in MeOH (7.8 mL) and paraformaldehyde (34 mg, 1.13 mmol) was added. Finally, $NaBH_3CN$ (35.6 mg, 0.57 mmol) was added. The crude was purified by flash chromatography using hexane/AcOEt (95:5) to give **18b** (43.5 mg, 0.11 mmol, 35 % over two steps) as a yellowish oil. IR (neat): 3437, 2923, 2853, 2360, 1735, 1457, 1374, 1231, 1025 cm^{-1}. ^1H NMR (400 MHz, CD_3OD) δ 4.57 (s, 1H), 4.24–4.10 (m, 2H), 2.49 (s, 6H), 2.30–2.14 (m, 2H), 1.99–1.90 (m, 2H), 1.57–1.20 (m, 25H), 0.97–0.84 (m, 6H). ^{13}C NMR (100 MHz, CD_3OD) δ 173.5, 87.9, 79.8, 71.2, 68.1, 62.0, 50.2, 33.1, 30.8, 30.5, 30.3, 29.9, 29.7, 26.2, 23.8, 19.4, 14.6, 14.5, 8.7. HR ESI-TOF MS Calculated for [M + H^+] $C_{24}H_{47}N_2O_3^+$ (*m/z*): 411.3581; found: 411.3588.

4.1.30. rac-(2R,3S)-2-(2,2-dimethylhydrazinyl)-2-ethyloctadec-4-yne-1,3-diol (19b)

Following the general procedure to obtain alcohols, **18b** (45.5 mg,

0.11 mmol) was treated with a solution of DIBAL (0.28 mL, 1 M in dichloromethane, 0.28 mmol) in CH_2Cl_2 (0.28 mL). The crude was purified by silica gel chromatography using $CHCl_3$:MeOH:NH_4OH (99.5:0.5:0.1) to afford **19b** (17.6 mg, 0.05 mmol, 43 %) as a yellow oil. IR (neat): 3305, 2923, 2853, 2775, 2358, 2320, 1464, 1045 cm^{-1}. ^1H NMR (400 MHz, CD_3OD) δ 4.54 (t, $J = 2.1$ Hz, 1H), 3.80 (d, $J = 11.0$ Hz, 1H), 3.65 (d, $J = 11.0$ Hz, 1H), 2.51 (s, 6H), 2.26 (td, $J = 6.8$, 2.1 Hz, 2H), 1.68–1.38 (m, 6H), 1.31 (bs, 19H), 0.97–0.88 (m, 6H). ^{13}C NMR (100 MHz, CD_3OD) δ 87.9, 80.1, 67.6, 64.7, 63.7, 50.5, 33.1, 30.8, 30.7, 30.5, 30.3, 29.9, 29.8, 25.1, 23.8, 19.4, 14.5, 7.8. HR ESI-TOF MS for [M + H^+] $C_{22}H_{45}N_2O_2^+$ (*m/z*): 369.3476; found: 369.3475.

4.1.31. Ethyl rac-(2R,3R,4E)-2-(2,2-dimethylhydrazinyl) −3-hydroxy-2-ethyloctadec-4-enoate (20b)

The reaction was carried out following the general procedure for the synthesis of *N,N*-dimethyl hydrazines starting from **10b** (169.1 mg, 0.33 mmol) and methylhydrazine (25.8 μL, 0.49 mmol) in 2.4 mL of THF. After deprotection completion the resulting crude was dissolved in MeOH (9 mL) and paraformaldehyde (39.4 mg, 1.31 mmol) was added. Finally, $NaBH_3CN$ (41.2 mg, 0.66 mmol) was added. The crude was purified by flash chromatography using hexane/Et_2O (4:1) to give **20b** (46.8 mg, 0.11 mmol, 35 % over two steps) as a yellow oil. IR (neat): 3450, 3387, 2954, 2853, 2366, 1731, 1465, 1225, 1024 cm^{-1}. ^1H NMR (400 MHz, $CDCl_3$) δ 5.85–5.49 (m, 2H), 4.27 (d, $J = 6.8$ Hz, 1H), 4.16 (q, $J = 7.1$ Hz, 2H), 2.50 (s, 6H), 2.03 (ddd, $J = 13.8$, 6.8, 3.0 Hz, 2H), 1.84 (qd, $J = 14.3$, 7.4 Hz, 2H), 1.36–1.17 (m, 25H), 0.90–0.81 (m, 6H). ^{13}C NMR (100 MHz, $CDCl_3$) δ 173.6, 134.5, 129.0, 78.0, 69.7, 61.0, 50.3, 32.6, 32.0, 29.8, 29.6, 29.5, 29.3, 26.7, 22.8, 14.3, 8.1. HR ESI-TOF MS for [M + H^+] $C_{24}H_{49}N_2O_3^+$ (*m/z*): 413.3738; found: 413.3750.

4.1.32. rac-(2R,3S,4E)-2-(2,2-dimethylhydrazinyl)-2ethyloctadec-4-ene-1,3-diol (21b)

Following the general procedure to obtain alcohols, **20b** (28 mg, 0.07 mmol) was treated with a solution of DIBAL (0.16 mL, 1 M in dichloromethane, 0.16 mmol) in CH_2Cl_2 (0.16 mL). The crude was purified by silica gel chromatography using hexane/AcOEt (4:1) to accomplish the sphingosine derivative **21b** (16.2 mg, 0.05 mmol, 67 %) as a yellowish oil. IR (neat): 3362, 3266, 2921, 2852, 2358, 2342, 1464, 1260, 1100, 1024, 802, 970 cm^{-1}. ^1H NMR (400 MHz, CD_3OD) δ 5.69 (dt, $J = 15.3$, 6.8 Hz, 1H), 5.57 (ddt, $J = 15.3$, 7.5, 1.1 Hz, 1H), 4.10 (d, $J = 7.5$ Hz, 1H), 3.66 (d, $J = 11.1$ Hz, 1H), 3.48 (d, $J = 11.1$ Hz, 1H), 2.49 (s, 6H), 2.06 (dd, $J = 14.0$, 6.8 Hz, 2H), 1.61–1.49 (m, 2H), 1.44–1.22 (m, 22H), 0.89 (t, $J = 7.1$, Hz, 3H), 0.88 (t, $J = 7.5$, Hz, 3H). ^{13}C NMR (100 MHz, CD_3OD) δ 134.8, 130.0, 77.3, 64.0, 63.2, 50.4, 33.4, 33.1, 30.8, 30.6, 30.5, 30.3, 30.2, 25.3, 23.8, 14.5, 7.9. HR ESI-TOF MS for [M + H^+] $C_{22}H_{47}N_2O_2^+$ (*m/z*): 371.3632; found: 371.3634.

4.1.33. Ethyl rac-(2R,3R)-2-(2,2-dimethylhydrazinyl)-3-hydroxy-2-ethyloctadecanoate (22b)

The reaction was carried out following the general procedure for the synthesis of *N,N*-dimethyl hydrazines starting from **11b** (183.3 mg, 0.36 mmol) and methylhydrazine (28.2 μL, 0.54 mmol) in 2.7 mL of THF. After deprotection completion the resulting crude was dissolved in 9.8 mL of MeOH and paraformaldehyde (42.6 mg, 1.42 mmol) was added. Finally, $NaBH_3CN$ (44.6 mg, 0.71 mmol) was added. The crude was purified by flash chromatography using hexane/Et_2O (87:13) to give **22b** (54.3 mg, 0.13 mmol, 37 % over two steps) as a yellow oil. IR (neat): 3368, 2923, 2852, 2773, 2365, 2327, 1466, 1276, 1054 cm^{-1}. ^1H NMR (400 MHz, $CDCl_3$) δ 4.15–3.98 (m, 2H), 3.76 (dd, $J = 10.2$, 1.9 Hz, 1H), 2.48 (s, 6H), 2.03–1.71 (m, 2H), 1.64–1.42 (m, 2H), 1.35–1.08 (m, 29H), 0.93–0.74 (m, 6H). ^{13}C NMR (100 MHz, $CDCl_3$) δ 174.1, 76.3, 69.4, 60.9, 50.3, 33.3, 32.0, 29.8, 29.7, 29.5, 26.8, 26.4, 22.8, 14.3, 14.2, 8.0. HR ESI-TOF MS Calculated for [M + H^+] $C_{24}H_{51}N_2O_3^+$ (*m/z*): 415.3894; found: 415.3882.

4.1.34. rac-(2R,3S)-2-(2,2-dimethylhydrazinyl)-2-ethyloctadecane-1,3-diol (23b)

Following the general procedure to obtain alcohols, **22b** (54.3 mg, 0.13 mmol) was treated with a solution of DIBAL (0.33 mL, 1 M in dichloromethane, 0.33 mmol) in CH_2Cl_2 (0.33 mL). The crude was purified by silica gel chromatography using hexane/AcOEt (3:2) to afford **23b** (44.6 mg, 0.12 mmol, 91 %) as a yellowish oil. IR (neat): 3368, 2923, 2852, 2773, 2365, 2326, 1465, 1054, 749 cm^{-1}. ^1H NMR (400 MHz, CD_3OD) δ 3.70 (d, $J = 10.9$ Hz, 1H), 3.60 (dd, $J = 10.3$, 1.5 Hz, 1H), 3.53 (d, $J = 10.9$ Hz, 1H), 2.46 (s, 6H), 1.66–1.40 (m, 4H), 1.40–1.22 (m, 26H), 0.92–0.79 (m, 6H). ^{13}C NMR (100 MHz, CD_3OD) δ 76.0, 64.2, 63.2, 50.5, 33.1, 32.4, 30.8, 30.5, 27.9, 25.3, 23.8, 14.5, 7.7. HR ESI-TOF MS for [M + H^+] $C_{22}H_{49}N_2O_2^+$ (*m/z*): 373.3789; found: 373.3782.

4.1.35. Ethyl (E)-octadec-2-ene-4-ynoate (4c)

The reaction was performed as described in general procedure to synthesize α,β-unsaturated esters *n*BuLi (2.6 M in hexane, 3.3 mL, 5.28 mmol), 1-pentadecyne (1.26 mL, 4.80 mmol), 1-formylpiperidine (0.6 mL, 5.38 mmol), triethyl phosphonoacetate (1.6 mL, 8.1 mmol), LiBr (1800 mg, 20.90 mmol), Et_3N (0.9 mL) to afford a mixture of two esteroisomers *cis/trans* (13:87). Purification by flash chromatography (hexane/Et_2O (95:5)) afforded product **4c** (1278.1 mg, 4.17 mmol, 58 % over two steps) as a yellowish oil. IR (neat): 2922, 2853, 2358, 2214, 1716, 1619, 1465, 1299, 1155, 1035, 630 cm^{-1}. ^1H NMR (400 MHz, $CDCl_3$) δ 6.74 (dt, $J = 15.8$, 2.2 Hz, 1H), 6.12 (d, $J = 15.8$ Hz, 1H), 4.19 (q, $J = 7.1$ Hz, 2H), 2.35 (td, $J = 7.0$, 2.2 Hz, 2H), 1.66–1.46 (m, 2H), 1.43–1.32 (m, 2H), 1.32–1.17 (m, 21H), 0.87 (t, $J = 6.8$ Hz, 3H). ^{13}C NMR (100 MHz, $CDCl_3$) δ 166.3, 129.4, 126.3, 101.0, 78.0, 60.7, 32.1, 29.8, 29.6, 29.5, 29.2, 29.0, 28.5, 22.8, 19.9, 14.4, 14.3. HR ESI-TOF MS for [M + Na^+] $C_{20}H_{34}NaO_2^+$ (*m/z*): 329.2451; found: 329.2458.

4.1.36. Ethyl rac-(2R,3S)-[1-(1,3-dioxo-1,3-dihydro-2H-isoindol-2-yl)- 3-(pentadec-1-yn-1-yl)aziridine]-2-carboxylate (6c)

Compound **4c** (1278.1 mg, 4.17 mmol) was treated with *N*-aminophthalimide (1352 mg, 8.34 mmol) and (diacetoxy)iodobenzene (2014 mg, 6.26 mmol) following the general procedure for aziridination. After the work-up, the crude was purified) to afford **6c** as a mixture of invertomers (78:22) (1128.6 mg, 2.41 mmol, 88 %) as a white solid. M. p. 63 °C. IR (neat): 2924, 2853, 2360, 2290, 1724, 1373, 1222, 1190, 891, 708, 632 cm^{-1}. ^1H NMR (400 MHz, $CDCl_3$) δ 7.80 (major, dd, $J = 5.5$, 3.0 Hz, 1.56H), 7.75 (minor, dd, $J = 5.5$, 3.0 Hz, 0.44H), 7.70 (major, dd, $J = 5.5$, 3.0 Hz, 1.56H), 7.66 (minor, dd, $J = 5.5$, 3.0 Hz, 0.44H), 4.34–4.23 (major, m, 1.56H), 4.13 (minor, q, $J = 7.1$ Hz, 0.44H), 3.94 (major, d, $J = 4.8$ Hz, 0.78H), 3.79 (minor, dt, $J = 4.9$, 1.8 Hz, 0.22H_3), 3.42 (major, dt, $J = 4.8$, 1.9 Hz, 0.78H), 3.35 (minor, d, $J = 4.9$ Hz, 0.22H), 2.22 (minor, td, $J = 7.1$, 1.8 Hz, 0.44H), 2.01 (major, tt, $J = 6.9$, 1.9 Hz, 1.56H), 1.50 (minor, m, 0.44H), 1.43–0.93 (m, 35H), 0.86 (m, 4H). ^{13}C NMR (100 MHz, $CDCl_3$) δ 166.6, 165.4, 164.6, 164.3, 134.2, 134.1, 130.1, 123.2, 87.7, 85.3, 73.9, 71.9, 62.2, 62.1, 45.7, 45.5, 37.3, 37.1, 31.9, 29.7, 29.6, 29.5, 29.4, 29.1, 29.0, 28.9, 28.6, 28.2, 28.0, 22.7, 18.8, 18.6, 14.1, 13.9. HR ESI-TOF MS calculated for [M + Na^+] $C_{28}H_{38}N_2NaO_4^+$ (*m/z*): 489.2724; found: 489.2728.

4.1.37. Ethyl rac-(2R,3R)-2-((1,3-dioxo-1,3-dihydro-2H-isoindol-2-yl) amino)-3-hydroxy-octadec-4-ynoate (8c)

Compound **8c** was prepared following the general procedure for the ring-opening aziridines, starting from **6c** (750.0 mg, 1.61 mmol) and *p*-toluensulfonic acid (336.0 mg, 1.77 mmol). After the work-up, the crude was purified by flash chromatography by using hexane/AcOEt (form 9:1 to 4:1). The desired product **8c** was obtained (351.1 mg, 0.72 mmol, 45 %) as a yellow solid. M.p. 83 °C. IR (neat): 3444, 3242, 2922, 2852, 2359, 2341, 1746, 1709, 1465, 1200 cm^{-1}. ^1H NMR (400 MHz, $CDCl_3$) δ 7.85 (dd, $J = 5.4$, 3.1 Hz, 2H), 7.75 (dd, $J = 5.5$, 3.1 Hz, 2H), 5.55 (d, $J = 4.3$ Hz, 1H), 4.69 (ddt, $J = 11.2$, 4.1, 2.0 Hz, 1H), 4.40–4.21 (m, 2H), 4.08 (d, $J = 11.2$ Hz, 1H), 3.77 (t, $J = 4.2$ Hz, 1H), 2.18 (td, $J = 7.1$, 2.0

Hz, 2H), 1.55–1.40 (m, 2H), 1.39–1.15 (m, 23H), 0.87 (t, J = 6.9 Hz, 3H). ^{13}C NMR (100 MHz, $CDCl_3$) δ 169.0, 166.9, 134.7, 130.0, 123.9, 87.6, 76.6, 68.4, 63.2, 62.3, 32.1, 29.8, 29.7, 29.5, 29.3, 28.9, 28.6, 22.8, 18.8, 14.3. HR ESI-TOF MS Calculated for [M + Na^+] $C_{28}H_{40}N_2NaO_5^+$ (m/z): 507.2829; found: 507.2834.

4.1.38. Ethyl rac-(2R,3R)-3-hydroxy-2-(2-(propan-2-ylidene)hydrazinyl) octadec-4-ynoate (12c)

The reaction was carried out following the general procedure for the synthesis of hydrazones starting from **8c** (161.4 mg, 0.33 mmol) and methylhydrazine (26.3 μL, 0.50 mmol) in THF (2.5 mL). After filtration, the resulting crude was redissolved in 3 mL of acetone and the reaction was stirred until complete consumption of starting material. The crude was purified by flash chromatography using hexane/AcOEt (9:1 to 4:1) to give **12c** (109.2 mg, 0.276 mmol, 83 % over two steps) as a yellowish oil. IR (neat): 3433 2923, 2854, 2366, 1740, 1466, 1371, 1194, 1026 cm^{-1}. ^{1}H NMR (400 MHz, $CDCl_3$) δ 5.38 (d, J = 8.8 Hz, 1H), 4.76 (bs, 1H), 4.31–4.12 (m, 3H), 3.69 (bs, 1H), 2.17 (td, J = 7.0, 1.8 Hz, 2H, H_6), 1.92 (s, 3H,), 1.84 (s, 3H), 1.53–1.40 (m, 2H), 1.38–1.21 (m, 23H), 0.87 (t, J = 6.8 Hz, 3H). ^{13}C NMR (100 MHz, $CDCl_3$) δ 170.6, 149.9, 87.7, 77.0, 66.6, 63.5, 61.5, 32.1, 29.8, 29.7, 29.5, 29.3, 28.9, 28.7, 25.4, 22.8, 18.8, 16.0, 14.3. HR ESI-TOF MS Calculated for [M + H^+] $C_{23}H_{43}N_2O_3^+$ (m/z): 395.3268; found: 395.3257.

4.1.39. Ethyl rac-(2R,3R)-2-(2,2-dimethylhydrazinyl)-3-hydroxyoctadec-4-ynoate (18c)

The reaction was carried out following the general procedure for the synthesis of *N,N*-dimethyl hydrazines starting from **8c** (156.5 mg, 0.32 mmol) and methylhydrazine (25.5 μL, 0.48 mmol) in THF (2.4 mL). When the deprotection was complete, the resulting crude was dissolved in 8.9 mL of MeOH and paraformaldehyde (48.5 mg, 1.61 mmol) was added. Finally, $NaBH_3CN$ (121.8 mg, 1.96 mmol) was added. The crude was purified by flash chromatography using hexane/AcOEt (95:5 to 4:1) to give **18c** (25.2 mg, 0.07 mmol, 20 % over two steps) as a yellowish oil. IR (neat): 3315, 2923, 2853, 2363, 2328, 1735, 1645, 1457, 1027 cm^{-1}. ^{1}H NMR (400 MHz, $CDCl_3$) δ 4.79 (dt, J = 3.9, 2.0 Hz, 1H), 4.31–4.15 (m, 2H), 3.89 (d, J = 3.9 Hz, 1H), 2.51 (s, 6H), 2.20 (td, J = 7.1, 2.0 Hz, 2H), 1.54–1.42 (m, 2H), 1.40–1.20 (m, 23H), 0.89 (t, J = 6.9 Hz, 3H). ^{13}C NMR (100 MHz, $CDCl_3$) δ 170.1, 87.1, 77.6, 64.5, 63.9, 61.6, 47.8, 32.1, 29.8, 29.7, 29.5, 29.3, 29.0, 28.8, 22.8, 18.9, 14.3. HR ESI-TOF MS for [M + H^+] $C_{22}H_{43}N_2O_3^+$ (m/z): 383.6238; found: 383.6258.

4.2. In vitro SphK inhibitory activity evaluation

For inhibitory activity quantification of the compounds synthesized, Adapta™ Universal Kinase Assay (Invitrogen, Carlsbad, CA, USA) was used [53]. Inhibitors were dissolved in 100% DMSO at a final concentration of 50 mM (100X solution). Several dilutions were performed at 20, 15, 10, 8, 6, 4, 2, 1 and 0.5 mM also in DMSO. Compounds were then pre-diluted to 4X in 1X Kinase Buffer A provided in the kit and plated in Corning white round-bottom 384 microplates. Each sample was analysed in triplicate. The assay was performed following strictly the indications provided by the manufacturer. SphK1 and SphK2 were used at final concentrations of 0.025 ng/μl and 0.8 ng/μl. ATP present in the reaction was at 1 μM and sphingosine at 5 μM. The reaction was stopped after 60 min of reaction with 10 mM EDTA, 3.6 nM ADP tracer and 2 nM anti-ADP antibody.

TR-FRET was read after 30 min in a CLARIOstar microplate reader (BMG Labtech, Biogen Científica SL, Madrid, Spain) using the following parameters: Ex = 340 nm; Em1 = 620/10; Em2 = 665/10; delay = 100 μs; integration time = 200 μs; Focal height = 11 mm. All steps were developed at room temperature.

Results of each condition were calculated as ratio EM_{665nm}/EM_{620nm} and expressed as % of inhibition using the following expression:

$$\%\ \text{Inhibition} = \frac{(\text{Ratio}_{\text{sample}} - \text{Ratio}_{0\%\text{Inhibition}})}{(\text{Ratio}_{100\%\text{inhibition}} - \text{Ratio}_{0\%\text{inhibition}})}$$

IC_{50} of each compound was calculated fitting the data to a sigmoidal dose–response curve with variable slope.

4.3. Computational studies

4.3.1. Molecular modelling

The co-crystal structure of SphK1 with its substrate sphingosine (3VZB, chain A, resolution 2 Å) was used as a template to build a SphK2 homology model with MOE 2019 software [56] after sequence alignment. The latter revealed additional residues 1–170 and 394–513 in SphK2, from which residues 1 to 170 were deleted due to the absence of a suitable template. Additional residues 394–513 were also excluded from the model since they did not directly affect the sphingolipid binding regions and lacked a suitable template. Subsequently, the homology model was verified by Ramachandran plots, which showed only 4 outliners far from the binding site, not connecting with it. The three distinctively different residues in the binding pocket were reproduced by the homology model and led to essential changes in the J-channel. In this regard, the replacement of Met272 with Leu553 at the pocket throat also led to a change in the position of identical residue Phe192, altering the shape of the J-channel. Further residue difference Ala339 in SphK1, corresponding to a Thr620 in SphK2, might also be relevant for the selectivity of potential ligands targeting the J-channel. This residue lies in the polar region and its variation affects a network of polar interactions that engage with the inhibitors.

4.3.2. Molecular docking

The crystal structure of SphK1 (3vzb) and the SphK2 homology model were prepared for docking with the MOE software using the Protein preparation protocol. One water molecule was kept in the SphK1 protein preparation process since it was found in all available X-ray crystal structures, forming H-bonds with Ser168, Gly342 and the respective ligand. For the homology model of SphK2, the water molecule was omitted, considering a difference with respect to SphK1 residue Ala339 (Thr620 in SphK2), which was found by the homology model to displace the water molecule from its interactions with Ser334 and the Gly623. Both enantiomers (2*R*,3*S*) and (2*S*,3*R*) of the designed compounds were drawn in MOE and underwent ligand preparation using Corina version 4.3.0 software [60], openbabel 3 version 3.0.0 [61] and ChemAxon software [62]. Additionally, the corresponding unsynthesized compounds, (**13c**, **19c**, and **21c**), with a trisubstituted center at C-2 were also prepared for docking. After the preparation steps, the rDock software [63] was used for cavity generation, using the co-crystal sphingosine substrate as a reference ligand. Subsequently, the designed molecules were docked in the generated binding pocket with rDock, using permissive pharmacophoric restraints to ensure that the polar heads of the ligands remain in the polar region.

4.4. Toxicological studies

4.4.1. Cell culture

Human umbilical vein endothelial cells (HUVEC) were isolated by collagenase treatment [64] and maintained in human endothelial cell specific medium (EBM-2, Lonza, Barcelona, Spain), supplemented with endothelial growth media (EGM-2, Lonza) and containing 10% fetal bovine serum (FBS, Biowest, Nuaillé, France). Cells were grown to confluence up to passage 1 to preserve endothelial features. Prior to every experiment, cells were incubated for 24 h in medium containing 1% FBS for apoptosis and 0.1% for MTT assays.

4.4.2. Cytotoxicity assay

A 100 μL suspension of HUVECs in supplemented RPMI medium (2

$\times 10^{5n}$cells/mL) was added to each well of a 96-well microtiter plate. Cells in 0.1% FBS supplemented EBM-2 medium (Lonza, Verviers, Belgium) were incubated in the absence or presence of compounds **19a** and **19b** (10, 30 and 100 μM) at 37 °C for 24 h. 3-(4,5-Dimethylthiazol-2-yl)-2,5-diphenyltetrazolium bromide (MTT, Sigma-Aldrich, Saint Louis, MO) was freshly prepared at 3 mg/mL in PBS, and 100 μL of MTT solution was added to each well followed by incubation at 37 °C for 3 h. The supernatants were discarded and 200 μL of DMSO was added to each well to dissolve the formazan product. The optical density at dual wavelengths (560 and 630 nm) was determined in a spectrophotometer (Infinite M200, Tecan, Mannedorf, Switzerland).

4.4.3. Cell apoptosis and survival assay

HUVEC cells were cultured on a 12-well plate and incubated in the absence or presence of compounds **19a** and **19b** (10, 30 and 100 μM) for 24 h in 1% FBS supplemented EBM-2 medium (Lonza) as described previously [65]. Then, cells were detached with StemPro Accutase cell dissociation reagent (5 min at 37 °C, Gibco, Thermo Fisher Scientific, Waltham, MA) and recovered by centrifugation (1400 rpm, for 10 min at 4 °C). Cells were resuspended in Annexin V Binding Buffer to obtain 1×10^5 cells in a final volume of 100 μL. Samples were incubated with 5 μL of FITC-Annexin V and 5 μL of propidium iodide (PI) from FITC Annexin V Detection Kit I (BD Biosciences, Franklin Lakes, NJ) for 15 min at room temperature in the dark following the manufacturer instructions and as previously described [66]. Cells were analyzed in a flow cytometer (BD Fortessax20, BD Biosciences, San Jose, CA) and differentiated as early apoptotic (annexin V+ and PI−), late apoptotic and/or necrotic (annexin V+ and PI+), and viable nonapoptotic (annexin V− and PI−) cells.. Results are presented as percentage of apoptotic and viable cells.

4.4.4. Statistical analysis

Differences between two groups were determined using an unpaired Student's *t* test. Values were expressed as mean ± SEM. Data were considered statistically significant when p values were <0.05.

Declaration of Competing Interest

The authors declare that they have no known competing financial interests or personal relationships that could have appeared to influence the work reported in this paper.

Acknowledgements

Financial support by the Ministerio de Economia y Competividad (Mineco), Spain (CTQ2014-58664-R and CTQ2017-89750-R), the Ministerio de Ciencia e Innovación, Spain (RTI2018-096429-B-I00), the Ministerio de Ciencia e Innovación, Spain [grant number SAF2017-89714-R, PID2020-120336RB-I00], the Generalitat Valenciana [PROMETEO/2019/032,] and the European Regional Development Fund are gratefully acknowledged. M.C.-M., A.G, and E.D acknowledge the Ministerio de Educación (predoctoral FPU fellowship FPU14/02790), the URV and the Generalitat Valenciana, respectively, for their predoctoral grants. We also thank Prof. Alois Fürstner for allowing us to use his laboratory for the selective reduction of alkynes to *trans* alkenes and Dr. Alexandre Guthertz for providing us with the Ru catalyst.

Appendix A. Supplementary material

Supplementary data to this article can be found online at https://doi.org/10.1016/j.bioorg.2022.105668.

References

[1] a) M. Airola and Y. A. Hannun, Sphingolipid metabolism and neutral sphingomyelinases, Handb. Exp. Pharmacol. 215 (2013) 57−76; b) D. Corda and M. A. De Matteis, Lipid signalling in health and disease, FEBS Journal 280 (2013) 6280; c) S. A. Morad and M. C. Cabot, Ceramide-orchestrated signalling in cancer cells, Nat. Rev. Cancer 13 (2013) 51−65; d) K. A. Orr Gandy and L. M. Obeid, Targeting the Sphingosine Kinase/Sphingosine 1-Phosphate Pathway in Disease: Review of Sphingosine Kinase Inhibitors, Biochim. Biophys. Acta 1831 (2013) 157−166; e) T. S.Tirodkar and C. Voelkel-Johnson, Sphingolipids in apoptosis, Exp. Oncol. 34 (2012) 231−242; f) Y.A. Hannun, L.M Obeid, Principles of bioactive lipid signalling: lessons from sphingolipids, Nature Rev. Mol. Cell Biol. 9 (2008) 139-150; g) C. E. Chalfant and S. Spiegel, Sphingosine 1-phosphate and ceramide 1-phosphate: expanding roles in cell signaling, J. Cell Sci. 118 (2005) 4605−4612; h) T. H. Kee, P. Vit and A. Melendez, Sphingosine kinase signalling in immune cells, J. Clin. Exp. Pharmacol. Physiol. 32 (2005) 153−161; i) S. Pyne and N. J. Pyne, Sphingosine 1-phosphate signalling in mammalian cells, Biochem. J. 349 (2000) 385−402.

[2] a) M. Z. Ratajczak, M. Suszynska, S. Borkowska, J. Ratajczak and G. Schneider, The role of sphingosine-1 phosphate and ceramide-1 phosphate in trafficking of normal stem cells and cancer cells, Expert. Opin. Ther. Targets 18 (2014) 95−107; b) B. Ogretmen and Y. A. Hannun, Biologically active sphingolipids in cancer pathogenesis and treatment, Nat. Rev. Cancer 4 (2004) 604−616; c) B. Ogretmen, Sphingolipids in cancer: Regulation of pathogenesis and therapy *FEBS Lett.* 580 (2006) 5467−5476.

[3] a) M.J. Pulkoski-Gross, J.C. Donaldson, L.M. Obeid, Sphingosine-1-phosphate metabolism: A structural perspective, Crit Rev. Biochem. Mol. Biol. 50 (2015) 298-313; b) G. T. Kunkel, M. Maceyka, S. Milstien and S. Spiegel, Targeting the sphingosine-1-phosphate axis in cancer, inflammation and beyond, Nat. Rev. Drug Discovery 12 (2013) 688−702; c) M. Maceyka, K.B. Harikumar, S. Milstien, S. Spiegel, Sphingosine-1-phosphate signaling and its role in disease, Trends Cell Biol. 22 (2012) 50-60; d) S. Spiegel and S. Milstein, The outs and the ins of sphingosine-1-phosphate in immunity, Nat. Rev. Immunol. 11 (2011), 403-415; e) H Fyrst, J. Saba, An update on sphingosine-1-phosphate and other sphingolipid mediators, Nat. Chem Biol. 6 (2010) 489-497; f) S. Pyne, J. Chapman, L. Steele and N. J. Pyne, Sphingomyelin-derived lipids differentially regulate the extracellular signal-regulated kinase 2 (ERK-2) and c-Jun N-terminal kinase (JNK) signal cascades in airway smooth muscle Eur. J. Biochem. 237 (1996) 819−826.

[4] O. Cuvillier, G. Pirianov, B. Kleuser, P. Vanek, O. Coso, J. Gutkind, S. Spiegel, Suppression of ceramide-mediated programmed cell death by sphingosine-1-phosphate, Nature 381 (1996) 800–803.

[5] N.C. Hait, C.A. Oskeritzian, S.W. Paugh, S. Milstein, S. Spiegel, Sphingosine kinases, sphingosine 1-phosphate, apoptosis and diseases, Biochim. Byophys. Acta 1758 (2006) 2016–2026.

[6] a) N.J. Pyne S. Pyne, Recent advances in the role of sphingosine 1-phosphate in cancer, FEBS Lett. 597 (2020) 3583-3601; b) N. J. Pyne, A. El Buri, D.R. Adams, S. Pyne, Sphingosine 1-phosphate and cancer, Adv. Biol. Regul. 68 (2018) 97-106; c) Bioactive sphingolipids in Cancer Biology and Therapy. Y.A. Hannun, C. Luberto, C. Mao, L.M. Obeid, (Eds.); Springer, 2015; d) N. J. Pyne and S. Pyne, Sphingosine 1-phosphate and cancer, Nat. Rev. Cancer 10 (2010) 489−503; e) J. Long, J. Edwards, C. Watson, S. Tovey, K. Mair, R. Schiff, V. Natarajan, N. J. Pyne and S. Pyne, Sphingosine Kinase 1 Induces Tolerance to Human Epidermal Growth Factor Receptor 2 and Prevents Formation of a Migratory Phenotype in Response to Sphingosine 1-Phosphate in Estrogen Receptor-Positive Breast Cancer CellsMol. Cell. Biol. 30 (2010) 3827−3841.

[7] J. Newton, S. Lima, M. Maceyka, S. Spiegel, Revisiting the sphingolipid rheostat: evolving concepts in cancer therapy, Exp. Cell Res. 333 (2015) 195–200.

[8] S.M. Pitson, Regulation of sphingosine kinase and sphingolipid signaling, Trends Biochem. Sci. 36 (2011) 97–107.

[9] D.R. Adams, S. Pyne, N.J. Pyne, Sphingosine Kinases: Emerging Structure-Function Insights, Trends Biochem. Sci. 41 (5) (2016) 395–409.

[10] (a) S. Spiegel, S. Milstien, Sphingosine 1-phosphate, a key cell signaling molecule, J. Biol. Chem. 277 (2002) 25851−25854; (b) S. M. Pitson, P. A. Moretti, J. R. Zebol, H. E. Lynn, P. Xia, M. A. Vadas, B. W. Wattenberg, Activation of sphingosine kinase 1 by ERK1/2-mediated phosphorylation, EMBO J. 22 (2003) 5491−5500; (c) S. M. Pitson, P. Xia, T. M. Leclercq, P. A. Moretti, J. R. Zebol, H. E. Lynn, P. Xia, B. W. Wattenberg, M. A. Vadas, Phosphorylation-dependent translocation of sphingosine kinase to the plasma membrane drives its oncogenic signalling J. Exp. Med. 201 (2005) 49−54; (d) S. Spiegel and S. Milstein, Sphingosine-1-phosphate: an enigmatic signalling lipid, Nat. Rev. Mol. Cell. Biol. 4 (2003) 397−407; (e) B. W. Wattemberg, S. M. Pitson and D. M. Raben, The sphingosine and diacylglycerol kinase superfamily of signaling kinases: localization as a key to signaling function, J. Lipid Res. 47 (2006) 1128−1139.

[11] (a) M. Maceyka, H. Sankala, N.C. Hait, H. Le Stunff, H. Liu, R. Toman, C. Collier, M. Zhang, L. S. Satin, A. H. Merrill, S. Milstien, S. Spiegel, SphK1 and SphK2, Sphingosine Kinase Isoenzymes with Opposing Functions in Sphingolipid Metabolism, J. Biol. Chem. 280 (2005) 37118–37129; (b) J. E. Chipuk, G. P. McStay, A. Bharti, T. Kuwana, C. J. Clarke, L. J. Siskind, L. M. Obeid, D. R. Green, Sphingolipid Metabolism Cooperates with BAK and BAX to Promote the Mitochondrial Pathway of Apoptosis, Cell 148 (2012) 988–1000.

[12] A. Olivera, T. Kohama, L. Edsall, V. Nava, O. Cuvillier, S. Poulton, S. Spiegel, Sphingosine Kinase Expression Increases Intracellular Sphingosine-1-phosphate and Promotes Cell Growth and Survival, J. Cell Biol. 147 (1999) 545–557.

[13] (a) H. Furuya, Y. Shimizu, P. M. Tamashiro, K. Iino, J. Bielawski, O.T.M. Chan, I. Pagano, T. Kawamori, Sphingosine kinase 1 expression enhances colon tumor growth, J. Transl. Med. 15 (2017) 120, (b) N.J. Pyne, F. Tonelli, K.G. Lim, J. Long, J. Edwards, S. Pyne, Targeting sphingosine kinase 1 in cancer, Adv. Enzym. Regul. 52 (2012) 31–38.

[14] (a) L. Hasanifard, R. Sheervalilou, M. Majidinia, B. Yousefi, New insights into the roles and regulation of SphK2 as a therapeutic target in cancer chemoresistance, J. Cell. Physiol. 234 (2019) 8162–8181; (b) N.J. Pyne, D.R. Adams, S. Pyne, Sphingosine Kinase 2 in Autoimmune/Inflammatory Disease and the Development

of Sphingosine Kinase 2 Inhibitors, Trends Pharmacol. Sci. 38 (2017) 581–591; (c) H.A. Neubauer, S.M. Pitson, Roles, regulation and inhibitors of sphingosine kinase 2, FEBS J. 280 (2013) 5317–5336.

[15] T. Okada, G. Ding, H. Sonoda, T. Kajimoto, Y. Haga, A. Khosrowbeygi, S. Gao, N. Miwa, S. Jahangeer, Nakamura, Involvement of N-terminal-extended Form of SphingosineKinase 2 in Serum-dependent Regulation of Cell Proliferation and ApoptosisJ, Biol. Chem. 280 (2005) 36318–36325.

[16] K.J. French, Y. Zhuang, L.W. Maines, P. Gao, W. Wang, V. Beljanski, J.J. Upson, C. L. Green, S.N. Keller, C.D. Smith, Pharmacology and Antitumor Activity of ABC294640, a Selective Inhibitor of Sphingosine Kinase-2, J. Pharmacol. Exp. Ther. 333 (1) (2010) 129–139.

[17] J.K. Venkata, N. An, R. Sturat, L.J. Costa, H. Cai, W. Coker, J.H. Song, K. Gibbs, T. Matson, E. Garrett-Mayer, Z. Wan, B. Ogretmen, C. Smith, Y. Yang, Inhibition of sphingosine kinase 2 downregulates the expression of c-Myc and Mcl-1 and induces apoptosis in multiple myeloma, Blood 124 (2014) 1915–1925.

[18] Y. Kharel, M. Raje, M. Gao, A.M. Gellet, J.L. Tomsig, K.R. Lynch, W.L. Santos, Biochem. J. 447 (2012) 149–157.

[19] (a) D.J. Gustin, Y. Li, M.L. Brown, X. Min, M.J. Schmitt, M. Wanska, X. Wang, R. Connors, S. Johnstone, M. Cardozo, A.C. Cheng, S. Jeffries, B. Franks, S. Li, S. Shen, M. Wong, H. Wesche, G. Xu, T.J. Carlson, M. Plant, K. Morgenstern, K. Rex, J. Schmitt, A. Coxon, N. Walker, F. Kayser, Z. Wang, Structure guided design of a series of sphingosine kinase (SphK) inhibitors, Bioorg. Med. Chem. Lett. 23 (2013) 4608–4616; (b) J. Wang, S. Knapp, N.J. Pyne, S. Pyne, J.M. Elkins, Crystal Structure of Sphingosine Kinase 1 with PF-543, ACS Med. Chem. Lett. 5 (2014) 1329–1333; (c) Z. Wang, X. Min, S.H. Xiao, S. Johnstone, W. Romanow, D. Meininger, H. Xu, J. Liu, J. Dai, S. An, S. Thibault, N. Walker, Molecular Basis of Sphingosine Kinase 1 Substrate Recognition and Catalysis, Structure 21 (2013) 798–809.

[20] (a) T. Ding, Y. Zhi, W. Xie, Q. Yao, B. Liu, Rational design of SphK inhibitors using crystal structures aided by computer. Eur. J. Med. Chem 213 (2021) 113164; (b) D. R Adams, S. Pyne, N.J. Pyne, Structure-function analysis of lipid substrates and inhibitors of sphingosine kinases, Cell. Signal. 76 (2020) 109806; (c) J. Zhang, M. Zhang, J. Yu, Y. Shang, K. Jiang, Y. Jia, J. Wang, K. Yang, Investigating the binding mechanism of sphingosine kinase 1/2 inhibitors: Insights into subtype selectivity by homology modeling, molecular dynamics simulation and free energy calculation studies, J. Mol. Struct. 1208 (2020) 127900; (d) C.D. Sibley, E.A. Morris, Y. Kharel, A. M. Brown, T. Huang, D.R. Bevan, K.R. Lynch, W.L. Santos, Discovery of a Small Side Cavity in Sphingosine Kinase 2 that Enhances Inhibitor Potency and Selectivity, J. Med. Chem. 63 (2020) 1178–1198; (e) B.L. Worrell, A. M. Brown, W.L Santos, D.R. Bevan, In silico Characterization of Structural Distinctions Between Isoforms of Human and Mouse Sphingosine Kinases for Accelerating Drug Discovery, J. Chem. Inf. Model. 59 (2019) 2339–2351; (f) D. R. Adams, S. Tawati, G. Berreta, P. Lopez Rivas, J. Baiget, Z. Jiang, A. Alsfouk, S. P. Mackay, N. J. Pyne, S. Pyne, Topographical Mapping of Isoform-Selectivity Determinants for J-Channel-Binding Inhibitors of Sphingosine Kinases 1 and 2, J. Med. Chem. 62 (2019) 3658–3676; (g) P. Gao, Y.K. Peterson, R.A. Smith, C. D. Smith, Characterization of Isoenzyme-Selective Inhibitors of Human Sphingosine Kinases, PLoS One 7 (2012) e44543.

[21] See reviews on sphingosine kinase inhibitors: (a) M.R. Pitman, M. Costabile, S.M. Pitson, Recent advances in the development of sphingosine kinase inhibitors, Cell. Signal. 28 (2016) 1349–1363; (b) K.R. Lynch, B. Thorpe and W.L. Santos, Sphingosine kinase inhibitors: a review of patent literature (2006–2015), Expert Opin. Ther. Pat. 26 (2016) 1409–1416; (c) P. Sanllehí, J. Abad, J. Casas, A. Delgado, Inhibitors of sphingosine-1-phosphate metabolism (sphingosine kinases and sphingosine-1-phosphate lyase), Chem. Phys. Lipids 197 (2016) 69–81; (d). W. L. Santos, K.R. Lynch, Drugging Sphingosine Kinases, ACS Chem. Biol. 10 (2015) 225–233; (e) D. Plano, S. Amin, A.K. Sharma, Importance of Sphingosine Kinase (SphK) as a Target in Developing Cancer Therapeutics and Recent Developments in the Synthesis of Novel SphK Inhibitors, J. Med. Chem. 57 (2014) 5509–5524; (f) D. Canals, Y.A. Hannun, Novel Chemotherapeutic Drugs in Sphingolipid Cancer Research, in: E. Gulbins, I. Petrache (Eds.), Sphingolipids: Basic Science and Drug Development. Handbook of Experimental Pharmacology, vol 215, Springer, Vienna, 2013, pp. 211−238; (g) S. Pyne, R. Bittman, N. Pyne, Perspective Sphingosine Kinase Inhibitors and Cancer: Seeking the Golden Sword of Hercules, Cancer Res. 71 (2011) 6576–6582; (h) P. Gangoiti, L. Camacho, L. Arana, A. Ouro, M. Granado, L. Brizuela, J. Casas, G. Fabriás, J Abad, A. Delgado, A. Gómez-Muñoz, Control of metabolism and signaling of simple bioactive sphingolipids: Implications in disease, Prog. Lipid Res. 49 (2010) 316–334; (i) A. Delgado, J. Casas, A. Llebaria, J. Abad, G. Fabrias, Inhibitors of sphingolipid metabolism enzymes, Biochim. Biophys. Acta 1758 (2006) 1957–1977.

[22] T. Ubai, H. Azuma, Y. Kotake, T. Inamoto, K. Takahara, Y. Ito, S. Kiyama, T. Sakamoto, S. Horie, S. Muto, S. Takahara, Y. Otsuki, Y. Katsuoka, FTY720 Induced Bcl-associated and Fas-independent Apoptosis in Human Renal Cancer Cells In Vitro and Significantly Reduced In Vivo Tumor Growth in Mouse Xenograft, Anticancer Res. 27 (2007) 75–88.

[23] K.G. Lim, F. Tonelli, E. Berdyshev, I. Gorshkova, T. Leclercq, S.M. Pitson, R. Bittman, S. Pyne, N.J. Pyne, Inhibition kinetics and regulation of sphingosine kinase 1 expression in prostate cancer cells: functional differences between sphingosine kinase 1a and 1b, Int. J. Biochem. Cell Biol. 44 (2012) 1457–1464.

[24] Y. Xiang, B. Hirth, J.L. Kane, J. Liao, K.D. Noson, C. Yee, G. Asmussen, M. Fitzgerald, C. Klaus, Booker, Discovery of novel sphingosine kinase-1 inhibitors. Part 2, Bioorg. Med. Chem. Lett. 20 (2010) 4550–4554.

[25] T.P. Mathews, A.J. Kennedy, Y. Kharel, P.C. Kennedy, O. Nicoara, M. Sunkara, A. J. Morris, B.R. Wamhoff, K.R. Lynch, T.L. Macdonald, Discovery, Biological Evaluation, and Structure-Activity Relationship of Amidine Based Sphingosine Kinase Inhibitors, J. Med. Chem. 53 (2010) 2766–2778.

[26] M.E. Schnute, M.D. McReynolds, T. Kasten, M. Yates, G. Jerome, J.W. Rains, T. Hall, J. Chrencik, M. Kraus, C.N. Cronin, M. Saabye, M.K. Highkin, R. Broadus, S. Ogawa, K. Cukyne, L.E. Zawadzke, V. Peterkin, K. Iyanar, J.A. Scholten, J. Wendling, H. Fujiwara, O. Nemirovskiy, A.J. Wittwer, M.M. Nagiec, Modulation of cellular S1P levels with a novel, potent and specific inhibitor of sphingosine kinase-1, Biochem. J. 444 (2012) 79–88.

[27] K. Liu, T.L. Guo, N.C. Hait, J. Allegood, H.I. Parikh, W. Xu, G.E. Kellogs, S. Grant, S. Spiegel, S. Zhang, Biological Characterization of 3-(2-amino-ethyl)-5-[3-(4-butoxyl-phenyl)-propylidene]-thiazolidine-2,4-dione (K145) as a Selective Sphingosine Kinase-2 Inhibitor and Anticancer Agent, PloS One 8 (2013) e56471.

[28] (a) K.G. Lim, C. Sun, R. Bittman, N.J. Pyne, S. Pyne, (*R*)-FTY720 methyl ether is a specific sphingosine kinase 2 inhibitor: Effect on sphingosine kinase 2 expression in HEK 293 cells and actin rearrangement and survivial of MCF-7 breast cancer cells, Cel. Signal. 23 (2011) 1590–1595; (b) G. Lim, F. Tonelli, Z. Li, X. Lu, R. Bittman, S. Pyne and N. J. Pyne, FTY720 analogues as sphingosine kinase 1 inhibitors: enzyme inhibition kinetics, allosterism, proteasomal degradation and actin rearrangement in MCF-7 breast cancer cells, J. Biol. Chem. 286 (2011) 18633–18640.

[29] (a) H. Li, C.D. Sibley, Y. Kharel, T. Huang, A.M. Brown, L.G. Wonilowicz, D.R. Bevan, K.R. Lynch, W.L. Santos, Lipophilic tail modifications of 2-(hydroxymethyl) pyrrolidine scaffold reveal dual sphingosine kinase 1 and 2 inhibitors, Bioorg. Med. Chem. 30 (2021) 115941; (b) M Vettorazzi, L.Vila, S. Lima, L. Acosta, F. Yépes, A. Palma, J. Cobo, J. Tegler, I. Malik, S. Alvarez, P. Marqués, N. Cabedo, M.J. Sanz, J. Jampilek, S. Spiegel, R.E. Enriz, Synthesis and biological evaluation of sphingosine kinase 2 inhibitors with anti-inflamatory activity, Arch. Pharm. Chem. Life Sci. 352 (2019) e1800298; (c) H. Ohno, M. Honda, N. Hamada, J. Miyagaki, A. Iwata, K. Otsuki, T. Maruyama, S. Nakamura, I. Nakanishi, S. Inuki, N. Fujii, S. Oishi, Identification of selective inhibitors of sphingosine 1 and 2 through a structure-activity relationship study of 4-epi-jaspine B, Bioorg. Med. Chem. 25 (2017) 3046–3052.

[30] (a) M. Congdon, R.G. Fritzemeier, Y. Kharel, A. M. Brown, V. Serbulea, D.R. Bevan, K.R. Lynch, W.L. Santos, Probing the substitution pattern of indole-based scaffolds reveals potent and selective sphigosine kinase inhibitors, Eur. J. Med. Chem. 212 (2021) 113121; (b) V.K. Reddy Tangadanchu, H. Jiang, Y. Yu, T.J.A. Graham, H. Liu, B.E. Rogers, R.Gropler, J. Perlmutter, Z. Tu, Structure-activity relationship studies and bioactivity evaluation of 1,2,3-triazole containing analogues as a selective sphingosine kinase-2 inhibitors, Eur. J. Med. Chem. 206 (2020) 112713; (c) E.S Childress, Y. Kharel, A. M. Brown, D.R. Bevan, K.R. Lynch, W.L. Santos, Transforming sphigosine kinase 1 inhibitors into dual and sphingosine kinase 2 selective inhibitors: design, synthesis and in vivo activity, J. Med. Chem. 60 (2017) 3933–3957; (d) M. D. Congdon, Y. Kharel, A. M. Brown, S. N. Lewis, D. R. Bevan, K. Lynch and W.L Santos, Structure−Activity Relationship Studies and Molecular Modeling of Naphthalene-Based Sphingosine Kinase 2 Inhibitors, ACS Med. Chem. Lett. 7 (2016) 229−234; (e) Y. Kharel, E.A. Morris, M.D. Congdon, S.B. Thorpe, J. L. Tomsig, W.L. Santos, K.R. Lynch, Sphingosine Kinase 2 Inhibition and Blood Sphingosine 1-Phosphate Levels J. Pharmacol. Exp. Ther. 355 (2015) 23–31; (f) M. D.Congdon, E.S. Childress, N.N. Patwardhan, J. Gumkowski, E. A. Morris, Y. Kharel, K.R. Lynch, W.L. Santos, Structure–activity relationship studies of the lipophilic tail region of sphingosine kinase 2 inhibitors, Bioorg. Med. Chem. Lett. 25 (2015) 4956–4960; (g) N.N. Patwardhan, E.A. Morris, Y. Kharel, M.R. Raje, M. Gao, J.L. Tomsig, K.R Lynch, W.L. Santos, Structure−Activity Relationship Studies and in Vivo Activity of Guanidine-Based Sphingosine Kinase Inhibitors: Discovery of SphK1- and SphK2-Selective Inhibitors J. Med. Chem. 58 (2015) 1879–1899; (h) Y. Kharel, M. Raje, M. Gao, A. Gellet, J.L. Tomsig, K.R. Lynch, W.L. Santos, Sphingosine kinase type 2 inhibition elevates circulating sphingosine 1-phosphate, Biochem. J. 447 (2012) 149–457.

[31] (a) J. D. Houck, T. K. Dawson, A. J. Kennedy, Y. Kharel, N. D. Naimon, S. D. Field, K. R. Lynch and Macdonald, Structural Requirements and Docking Analysis of Amidine-Based Sphingosine Kinase 1 Inhibitors Containing Oxadiazoles, ACS Med. Chem. Lett., 7 (2016) 487−492. (b) A. J. Kennedy, T.P. Mathews, Y. Kharel, S.D. Field, M. L. Moyer, J.E. East, J.D. Houck, K.R. Lynch, T.L. MacDonald, Development of Amidine-Based Sphingosine Kinase 1 Nanomolar Inhibitors and Reduction of Sphingosine 1-Phosphate in Human Leukemia Cells J. Med. Chem. 54 (2011) 3524–3548.

[32] (a) J. Llaveria, Y. Díaz, M.I. Matheu, S. Castillón, Enantioselective Synthesis of Jaspine B (Pachastrissamine) and Its C-2 and/or C-3 Epimers, Eur. J. Org. Chem. (2011) 1514–1519; (b) J.A. Morales-Serna, J. Llaveria, Y. Díaz, M.I. Matheu, S. Castillón, Recent advances in the synthesis of sphingosine and phytosphingosine, molecules of biological significance, Curr. Org. Chem. 14 (2010) 2483–2521; (c) J. A. Morales-Serna, O. Boutureira, A. Serra, M. I. Matheu, Y. Díaz; S. Castillón, Synthesis of Hyperbranched β-Galceramide-Containing Dendritic Polymers That Bind HIV-1 rgp120, Eur. J. Org. Chem. (2010) 2657–2660; (d) J. A. Morales-Serna; Y. Díaz; M. I. Matheu; S. Castillón, Efficient synthesis of ß-glycosphingolipids by reaction of stannylceramides with glycosyl iodides promoted by TBAI/AW 300 molecular sieves, Eur. J. Org Chem. (2009) 3849–3852; (e) J. Llaveria, Y. Díaz, M.I. Matheu, S. Castillón, An efficient and general enantioselective synthesis of sphingosine, phythosphingosine, and 4-substituted derivatives, Org. Lett. 11, (2009) 205–208; (f) J.A. Morales-Serna, Y. Díaz, M.I. Matheu, S. Castillón, Synthesis of D/L-erythro-Sphingosine Using a Tethered Aminohydroxylation Reaction as the Key Step, Synthesis (2009) 710–712; (g) J.A. Morales-Serna, J. Llaveria, Y. Díaz, M.I. Matheu, S. Castillón, Asymmetric sulfur ylide based enantioselective synthesis of D-erythro-sphingosine, Org. Biomol. Chem. 6 (2008) 4502–4504; (h) J. A. Morales-Serna, Y. Díaz, M. I. Matheu, S. Castillón, Stannyl Ceramides as Efficient Acceptors for Synthesising β-Galactosyl Ceramides, Org. Biomol. Chem. 6 (2008) 3831–3836; (i) J.A. Morales-Serna, O. Boutureira; Y. Díaz, M.I. Matheu, S. Castillón, Highly efficient and stereoselective synthesis of β-glycolipids, Org. Biomol. Chem. 6 (2008) 443–446; (j) O. Boutureira, J. A.

Morales-Serna, Y. Díaz, M. I. Matheu, S. Castillón, Direct and Efficient Glycosylation Protocol for Synthesizing α-Glycolipids: Application to the Synthesis of KRN7000, Eur. J. Org. Chem. (2008) 1851–1854; (k) J. A. Morales-Serna, O. Boutureira, Y. Díaz, M. I. Matheu, S. Castillón, Recent Advances in the Glycosylation of Sphingosines and Ceramides, Carbohydr. Res. 342 (2007) 1595–1612.

[33] M. Escudero-Casao, A. Cardona, R. Beltrán-Debón, Y. Díaz, M.I. Matheu, S. Castillón, Fluorinated triazole-containing sphingosine analogues. Syntheses and in vitro evaluation as SPHK inhibitors, Org. Biomol. Chem. 16 (39) (2018) 7230–7235.

[34] (a) Y. Igarashi, S. Hakomori, Enzymatic synthesis of N,N-dimethyl-sphingosine: Demonstration of the sphingosine: N-methyltransferase in mouse brain, Biochem. Biophys. Res. Commun. 164 (1989) 1411–1416; (b) O. Cuvillier, G. Pirianov, B. Kleuser, P.G. Vanek, O.A. Coso, S. Gutkind, S. Spiegel, Suppression of ceramide-mediated programmed cell death by sphingosine-1-phosphate. Nature 381 (1996) 800–803; (c) Y. Yatomi, F. Ruan, T. Megidish, T. Toyokuni, S. Hakomori, Y. Igarashi, *N,N*-dimethylsphingosine inhibition of sphingosine kinase and sphingosine-1-phospahte activity in human platelets. Biochemistry 35 (1996) 626–633; (d) H. Liu, M. Sugiura, V.E. Nava, L.C. Edsall, K. Kono, S. Poulton, S. Milstien, T. Kohama, S. Spiegel, Molecular cloning and functional characterization of a novel mammalian sphingosine kinase type 2 isoform. J. Biol. Chem. 275 (2000) 19513–19520.

[35] For contributions of our group on aziridination reactions, see: (a) I. Gimenez-Nueno, J. Guasch, I. Funes-Ardoiz, F. Maseras, M.I. Matheu, S. Castillon, Y. Diaz, Enantioselective Synthesis of 3-Heterosubstituted-2-amino-1-ols by Sequential Metal-Free Diene Aziridination/Kinetic Resolution, Chem. Eur. J. 25 (2019) 12628-12635; (b) J. Guasch, I. Giménez-Nueno, I. Funes-Ardoiz, M. Bernús, M.I. Matheu, F. Maseras, S. Castillón, Y. Díaz, Enantioselective Synthesis of Aminodiols by Sequential Rhodium-Catalysed Oxyamination/Kinetic Resolution: Expanding the Substrate Scope of Amidine-Based Catalysis, Chem. Eur. J. 24 (2018) 4635-4642; (c) J. Llaveria, A. Beltrán, W.M.C. Sameera, A. Locati, M.M. Díaz-Requejo, M. I. Matheu, S. Castillón, F. Maseras, P.J. Pérez, Chemo, Regio- and Stereoselective Silver-Catalyzed Aziridination of Dienes. Scope, Mechanistic Studies and Ring-Opening Reactions, J. Am Chem. Soc. 136 (2014) 5342-5350; (d) J. Guasch, Y. Díaz, M.I. Matheu, S. Castillón, Rhodium-catalyzed regio- and stereoselective oxyamination of dienes via tandem aziridination/ring-opening of dienyl carbamates, Chem. Commun. 55 (2014) 7344-7347; (e) I. Arenas, M. A. Fuentes, E. Álvarez, Y. Díaz, A. Caballero, S. Castillón, P.J. Pérez, Syntheses of a Novel Fluorinated Trisphosphinoborate Ligand and Its Copper and Silver Complexes. Catalytic Activity toward Nitrene Transfer Reactions, Inorg. Chem. (2014) 3991–3999; (f) J. Llaveria, A. Beltrán, M.M Díaz-Requejo, M.I. Matheu, S. Castillón, P.J. Pérez, Efficient Silver-Catalyzed Regio- and Stereospecific Aziridination of Dienes, Angew. Chem. Int. Ed. 49 (2010) 7092-7095.

[36] For reviews, see: (a) L. Degennaro, P. Trinchera and R. Luisi, Recent Advances in the Stereoselective Synthesis of Aziridines, Chem. Rev. 114 (2014) 7881-7929; (b) H. Ohno, Synthesis and Applications of Vinylaziridines and Ethynylaziridines , Chem. Rev.114 (2014) 7784-7814; (c) J. B. Sweeney, Aziridines: epoxides' ugly cousins?, Chem. Soc. Rev 31 (2002) 247-258; For reviews on asymmetric aziridination: (d) H. Pellisier, Recent Developments in Asymmetric Aziridination, Adv. Synth. Catal. 356 (2014) 1899-1935; (e) H. Pellissier, Recent developments in asymmetric aziridination, Tetrahedron 66 (2010) 1509; (f) P. Müller, C. Fruit, Enantioselective Catalytic Aziridinations and Asymmetric Nitrene Insertions into CH Bonds, Chem. Rev. 103 (2003) 2905-2919.

[37] The progress in the chemical synthesis of sphingosine and derivatives thereof has been reviewed in the last years: (a) see 32b; (b) Y. Gao, X. He, F. Ding, Y. Zhang, Recent Progress in Chemical Syntheses of Sphingosines and Phytosphingosines, Synthesis 48 (2016) 4017–4037.

[38] L. He, H.-S. Byun, R. Bittman, Stereoselective Preparation of Ceramide and Its Skeleton Backbone Modified Analogues via Cyclic Thionocarbonate Intermediates Derived by Catalytic Asymmetric Dihydroxylation of α, β-Unsaturated Ester Precursors, J. Org. Chem. 65 (22) (2000) 7627–7633.

[39] M.A. Kuznetsov, V.V. Semenovskii, V.N. Belov, V.A. Gidin, Reaction of phthalimidonitrene with phenylbutenynes, Chem. Heterocycl. Compd. 25 (1989) 136–142.

[40] J. Li, J.-L. Liang, P.W.H. Chan, C.-M. Che, Aziridination of alkenes with N-substituted hydrazines mediated by iodobenzene diacetate, Tetrahedron Lett. 45 (12) (2004) 2685–2688.

[41] L.B. Krasnova, R.M. Hili, O.V. Chernoloz, A.K. Yudin, C.V. Stevens, Phenyliodine (III) diacetate as a mild oxidant for aziridination of olefins and imination of sulfoxides with N-aminophthalimide, ARKIVOC IV 2005 (4) (2005) 26–38.

[42] (a) R. Akhtar, S. A R. Naqvi, A.F. Zahoor, S. Saleem, Nucleophilic ring opening reactions of aziridines, Mol. Div. 22 (2018) 447-501; (b) X.E. Hu, Nucleophilic ring opening of aziridines, Tetrahedron 60 (2004) 2701-2743; (c) I.D.G. Watson, A.K. Yudin, Ring-Opening Reactions of Nonactivated Aziridines Catalyzed by Tris (pentafluorophenyl)borane, J. Org. Chem. 68 (2003) 5160-5167.

[43] S. Chandrasekhar, C.H. Narsihmulu, S. Shameem Sultana, Ceric ammonium nitrate (CAN) catalyzed ring cleavage of N-tosyl aziridines: a potential tool for solution phase library generation, Tetrahedron Lett. 43 (41) (2002) 7361–7363.

[44] B. Sundararaju, A. Fürstner, A trans-Selective Hydroboration of Internal Alkynes, Angew. Chem. Int. Ed. 52 (52) (2013) 14050–14054.

[45] S.M. Rummelt, K. Radkowski, D.-A. Roşca, A. Fürstner, Interligand Interactions Dictate the Regioselectivity of trans-Hydrometalations and Related Reactions Catalyzed by [Cp*RuCl]. Hydrogen Bonding to a Chloride Ligand as a Steering Principle in Catalysis, J. Am. Chem. Soc. 137 (16) (2015) 5506–5519.

[46] K. Radkowski, B. Sundararaju, A. Fürstner, A Functional-Group-Tolerant Catalytic trans Hydrogenation of Alkynes, Angew. Chem. Int. Ed. 52 (2013) 355–360.

[47] S.M. Rummelt, A. Fürstner, Ruthenium-Catalyzed trans-Selective Hydrostannation of Alkynes, Angew. Chem. Int. Ed. 53 (14) (2014) 3626–3630.

[48] Non quaternized compounds were not reduced due to problems of retro-aldol reactions found in further derivatizations.

[49] N. Brosse, M.F. Pinto, J. Bodiguel, B. Jamart-Grégoire, A New Synthetic Route to Protected -Hydrazinoesters in High Optical Purity Using the Mitsunobu Protocol, J. Org. Chem. 66 (2001) 2869–2873.

[50] A. Alcaide, A. Trapero, Y. Pérez, A. Llebaria, Galacto configured N-aminoaziridines: a new type of irreversible inhibitor of β-galactosidases, Org. Biomol. Chem. 13 (2015) 5690–5697.

[51] Organic Photochromes, A. V. El'tsov (Ed.), Springer, New York, 1990.

[52] (a) M. Ayoub, J. Trebaux, J. Vallaghe, F. Charrier-Savournin, K. Al-Hosaini, A. Gonzalez Moya, J. Pin, K. Pfleger, E. Trinquet, Homogeneous time-resolved fluorescence-based assay to monitor extracellular signal-regulated kinase signaling in a high-throughput format, Front. Endocrinol. 5 (2014) 1–11; (b) T.A. Klink, K.M. Kleman-Leyer, A. Kopp, T.A. Westermeyer, R.G. Lowery, Evaluating PI3 Kinase Isoforms Using Transcreener™ ADP Assays, J. Biomol. Screen 13 (2008) 476-485.

[53] Adapta Universal Kinase Assay User Guide. Protocol part PV5099. Rev. 14 February 2008. Invitrogen.

[54] L. Wong, S.S.L. Tan, Y. Lam, A.J. Melendez, Synthesis and evaluation of sphingosine analogues as inhibitors of sphingosine kinases, J. Med. Chem. 52 (2009) 3618–3626.

[55] Note that both SphK1 and SphK2 have several isoforms and some authors refer to different isoforms. For clarity, we have used the residue numbering corresponding to the canonical isoform 1 for both proteins. SphK1: https://www.uniprot.org/uniprot/Q9NYA1#sequences. SphK2: https://www.uniprot.org/uniprot/Q9NRA0#sequences.

[56] Molecular Operating Environment (MOE), 2019.01; Chemical Computing Group ULC, 1010 Sherbooke St. West, Suite #910, Montreal, QC, Canada, H3A 2R7, 2021.

[57] X. Du, X. Xie, Y. Liu, Gold-catalyzed cyclization of alkynylaziridines as an efficient approach toward functionalized N-phth pyrroles, J. Org. Chem. 75 (2) (2010) 510–513.

[58] A. Fürstner, K. Radkowski, A chemo- and stereoselective reduction of cycloalkynes to (E)-cycloalkenes, Chem. Commun. (18) (2002) 2182–2183, https://doi.org/10.1039/B207169J.

[59] R. Bittman, N. J. Pyne, S. Pyne, D. J. Baek, Z. Liu and H. S. Byun, Selective inhibitors and allosteric activators of sphingosine kinase, WO 2014118556A2, 2014.

[60] Chemoinformatics ProgramPackage CORINA Classic, developed and distributed by Molecular Networks GmbH, Nuremberg, Germany and Altamira LLC, Columbus, OH, USA. www.mn-am.com.

[61] N.M. O'Boyle, M. Bank, C.A. James, C. Morley, T. Vandermeersch, G.R. Hutchison, Open Babel: An open chemical toolbox, J. Cheminformatics 3 (2011) 33.

[62] ChemAxon software was used for drawing, displaying and characterizing chemical structures, ChemAxon (https://www.chemaxon.com).

[63] S. Ruiz-Carmona, D. Alvarez-Garcia, N. Foloppe, A.B. Garmendia-Doval, S. Juhos, P. Schmidtke, X. Barril, R. Hubbard, S.D. Morley, rDock: A Fast, Versatile and Open Source Program for Docking Ligands to Proteins and Nucleic Acids. PLoS Comput. Biol. 10 (2014) e1003571.

[64] E.A. Jaffe, R.L. Nachman, C.G. Becker, C.R. Minick, Culture of Human Endothelial Cells Derived from Umbilical Veins. Identification by morphologic and immunologic criteria, J. Clin. Invest. 52 (1973) 2745–2756.

[65] M.T. Garcia, M.A. Blazquez, M.J. Ferrandiz, M.J. Sanz, N. Silva-Martin, J. A. Hermoso, A.G. de la Campa, J. Biol. Chem. 286 (2011) 6402–6413.

[66] M.C. Martin, I. Dransfield, C. Haslett, A.G. Rossi, New alkaloid antibiotics that target the DNA topoisomerase I of Streptococcus pneumonia, J. Biol. Chem. 276 (2001) 45041–45050.